NASA TECHNICAL MEMORANDUM

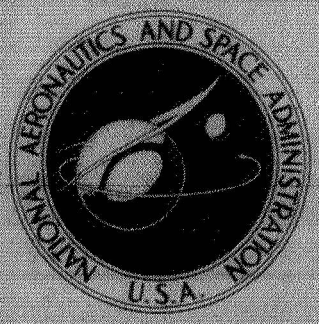

NASA TM X-2171

NASA TM X-2171

COOLING AIRFLOW THROUGH A STATIONARY TURBINE DISK AND BLADE

by Frederick C. Yeh, David J. Poferl, Reeves P. Cochran, and Hadley T. Richards

Lewis Research Center
Cleveland, Ohio 44135

NATIONAL AERONAUTICS AND SPACE ADMINISTRATION • WASHINGTON, D. C. • APRIL 1971

1. Report No.	2. Government Accession No.	3. Recipient's Catalog No.
NASA TM X-2171		

4. Title and Subtitle	5. Report Date
COOLING AIRFLOW THROUGH A STATIONARY TURBINE DISK AND BLADE	April 1971
	6. Performing Organization Code

7. Author(s)	8. Performing Organization Report No.
Frederick C. Yeh, David J. Poferl, Reeves P. Cochran, and Hadley T. Richards	E-6006
	10. Work Unit No. 720-03

9. Performing Organization Name and Address	11. Contract or Grant No.
Lewis Research Center National Aeronautics and Space Administration Cleveland, Ohio 44135	
	13. Type of Report and Period Covered Technical Memorandum

12. Sponsoring Agency Name and Address	14. Sponsoring Agency Code
National Aeronautics and Space Administration Washington, D.C. 20546	

15. Supplementary Notes

16. Abstract

The cooling-air pressure changes through a stationary turbine disk and blade assembly and the airflow distribution within a blade were determined experimentally. Tests were conducted with room-temperature air over a range of inlet pressures from 28 to 100 psia (19 to 69 N/cm^2) and flow rates from 0.12 to 0.45 lb/sec (0.055 to 0.20 kg/sec). Based on demonstrated agreement between measured and calculated rotor disk and blade pressures, an analytical procedure is proposed for predicting the cooling-air pressure changes through the rotor disk and blade during engine operation.

17. Key Words (Suggested by Author(s))	18. Distribution Statement
Turbine cooling Flow distribution Pressure distribution Labyrinth seal leakage	Unclassified - unlimited

19. Security Classif. (of this report)	20. Security Classif. (of this page)	21. No. of Pages	22. Price*
Unclassified	Unclassified	44	$3.00

*For sale by the National Technical Information Service, Springfield, Virginia 22151

COOLING AIRFLOW THROUGH A STATIONARY TURBINE DISK AND BLADE

by Frederick C. Yeh, David J. Poferl, Reeves P. Cochran,
and Hadley T. Richards

Lewis Research Center

SUMMARY

An analytical procedure is presented as a proposed method for predicting coolant flow pressure changes through a disk-blade flow path and coolant flow distribution through a specific radial-flow blade configuration under the conditions encountered in engine operation. This procedure is based on demonstrated agreement between calculated and experimentally measured pressure in static, isothermal tests. These tests were conducted to evaluated (1) leakage rates across a balanced-pressure labyrinth seal and through the serrated-blade mounting slots in the disk rim, (2) cooling-air pressure drops from the disk cooling-air inlet to the blade tip, and (3) coolant flow distribution at the blade tip. Labyrinth seal leakages were measured during room-temperature tests at pressures of 50 and 100 psia (34.5 and 69 N/cm^2). These leakages varied from 0.0095 to 0.04 pound per second (0.0043 to 0.018 kg/sec). Blade serration leakage for a five-blade test cascade was determined over a range of pressures from 20 to 100 psia (14 to 60 N/cm^2) and temperatures from 67° to 472° F (293 to 518 K). These serration leakages varied from 0.0011 to 0.018 pound per second (0.00050 to 0.0082 kg/sec). Pressure drops in the turbine disk passages were determined at room temperatures over a range of disk hub inlet cooling-air pressures from 28 to 100 psia (19 to 69 N/cm^2) and flow rates for the five-blade cascade from 0.12 to 0.45 pound per second (0.055 to 0.20 kg/sec). The pressure drops through a single blade were measured at room temperature for inlet pressures from 42 to 57 psia (29 to 39 N/cm^2). Coolant flow for the single-blade study varied from 0.0155 to 0.0475 pound per second (0.0070 to 0.0215 kg/sec). Flow distributions from the radial cooling passages of the blade were correlated with a pressure drop parameter for both constant pressures and chordwise pressure gradients across the blade tip.

INTRODUCTION

This report presents the results of a study to determine the cooling-air pressure drop and leakage through a stationary turbine rotor disk - blade assembly. Some tests involved leakages that occur along the cooling-air flow path between the hub of the turbine disk and the root of the turbine blade. Other tests were made to determine the flow distribution and pressure drop through the blade. This information will be applied to determine the coolant flow rate to the test blades in a turbojet engine used for turbine cooling research purposes at Lewis. The test-bed turbojet engine used in this program is described in detail in reference 1.

In order to obtain significant engine performance gains, the requirement for increased gas turbine-inlet temperatures and associated turbine component metal temperatures have pushed heat-resistant materials to the limit of their capabilities, even when these components are internally cooled. Therefore, if structural failure of critically stressed components is to be avoided, it is essential that turbine component metal temperatures be accurately predicted. For air-cooled turbine blade investigations the accurate determination of the cooling-air flow and pressure distributions through turbine blades is essential to the heat-transfer analysis required to accurately predict blade metal temperatures.

To investigate the flow characteristics of the engine turbine blade air supply system, an apparatus was used to position the various components of this system in the proper relative locations. Because of the difficulties involved in making and interpreting pressure measurements on a rotating turbine disk, it was desirable to investigate cooling-air flow and pressure drop characteristics in nonrotating tests. This apparatus was used to determine the following: (1) pressure drops in the cooling air from the disk inlet to the base of the turbine blade; (2) leakage rates of cooling air through the serrated-blade mounting slots at the rim of the disk; and (3) leakage rates across a balanced-pressure labyrinth seal at very small pressure differences. The cooling air pressure drop in turbine disk passages was investigated for room-temperature air over a range of disk hub inlet air pressures from 28 to 100 psia (19 to 69 N/cm^2). In another series of tests, serration leakages were measured at cooling-air temperatures from 67° to 472° F (293 to 518 K) and blade base pressures from 20 to 100 psia (14 to 69 N/cm^2). Labyrinth seal leakages were determined at room temperature for inlet pressures at the disk hub of 50 and 100 psia (34.5 and 69 N/cm^2).

For detailed studies of the flow characteristics of the blade only, static tests were conducted on a single blade in a flow apparatus over a range of conditions that simulated expected cooling-air pressure in the engine. Airflow rates ranged from 0.0155 to 0.0475 pound per second (0.0070 to 0.0215 kg/sec), inlet pressures ranged from 42 to 57 psia (20 to 39 N/cm^2), and the coolant temperature was 80° F (300 K). For one series of

tests, the leading-edge, midchord, and trailing-edge exit pressures at the blade tip were maintained equal. Constant-pressure levels of 44, 36, and 30 psia (30, 25, and 21 N/cm^2) were investigated. In order to determine the effect of chordwise pressure variation across the blade tip on flow distribution, blade tip gradients (from leading edge to trailing edge) of 40 to 32 psia (28 to 22 N/cm^2) and 43 to 27 psia (30 to 19 N/cm^2) were also investigated.

The blade flow characteristics from the disk-blade assembly and single-blade investigations are compared, and proposed procedures for using the data reported herein for analyzing rotating engine data are also presented.

RESEARCH ENGINE TEST BLADE COOLING-AIR SYSTEM

The test-bed turbojet research engine described in reference 1 is equipped with two cooling-air systems for the blades on the turbine disk. One of these systems provides cooling air to a rotating cascade of five adjacent test blades; the other system provides cooling air to the remaining "workhorse" or "slave" blades on the turbine disk. This dual cooling system permits variation of the coolant flow to the test blades independent of the slave blades, and an accurate determination of the cooling airflow to the test blades. This system then allows a variety of test blades to be investigated in the five-blade cascade with a minimum change in hardware on the turbine disk. The engine is designed to operate at a cooling-air flow rate of 0.04 pound per second (0.017 kg/sec) per blade.

The details of the test blade cooling-air system of the research engine are shown in figure 1. Cooling airflow is introduced into an annular manifold shown on the lower right of the figure. The cooling air flows through a series of holes in the forward wall of the annular manifold to enter chamber 2. The inner and outer radii of chamber 2 are bounded by three-stage balanced-pressure labyrinth seals. Twenty-four radial holes in the inner rear sideplate provide flow paths for the test blade cooling air to pass from chamber 2 to chamber 5. Chamber 5 is an annulus bounded by the turbine disk, the clamp ring, and the outer rear sideplate. Cooling air flows through a radial passage (chamber 6) under the outer rear sideplate in the circumferential location of the five test blades to the base of the blades (chamber 7). From chamber 7, the cooling air enters the blade, flows radially outward, and is discharged into the gas stream after flowing through the internal cooling passages of the blade. For this investigation, the blade configuration shown in figure 2 was used. This blade is a one-piece casting with an extended stalk root. The airfoil portion of the blade has a span of about 4 inches (10.2 cm) and a chord at midspan of about 1.6 inches (4.1 cm). The cooling-air passages in the blade consist of two radial slots in the stalk portion, a short transition

section between the stalk and the airfoil portions, and a hollow airfoil portion with radial fins on the inner surfaces of both the pressure and suction sides. These fins were of varying lengths, as shown in figure 2. Slotted ribs between the pressure and suction sides in the leading- and trailing-edge portions of the airfoil divide the flow area into three interconnected passages. There were 13 slots in each rib. These slots were 0.25 inch by 0.040 inch (0.63 cm by 0.10 cm) in the leading-edge rib and 0.25 inch by 0.03 inch (0.63 cm by 0.076 cm) in the trailing-edge rib.

The test blade cooling-air flow rate is measured at a venturi tube upstream of the disk inlet. Because of several possibilities for leakage either into or out of the test blade cooling-air flow passages, this measurement must be corrected to determine the exact amount of cooling air passing through the test blades. These potential leakage points are (1) between chambers 1 and 2 and between chambers 2 and 3 across the three-stage labyrinth seals; (2) between chamber 6 and the environment at the rear face of the turbine disk; and (3) between chamber 7 and the environments around the blade root serrations and at the forward face of the turbine disk. The quantity of air gained or lost by the cooling airflow at these potential leakage points can be approximated by experimental static room-temperature calibration at pressure levels and pressure differences between chambers that simulate engine operation.

During engine operation, pressure balances should be maintained between chambers 1 and 2 and between chambers 2 and 3. If these pressure balances were perfect, there would be no interchange of air between these chambers. However, it has been found during actual engine operation that these pressure balances can be held to within a fraction of an inch of water.

The thrust-balance chamber (chamber 4, fig. 1) is used on the engine to balance pressure loads imposed on the turbine disk by the gas stream and the various cooling airflows. The pressure in this chamber must be kept at a level below that in chamber 3 to ensure that there is a positive flow of air from chamber 3 to chamber 4 to accomplish the pressure-balance function of the outer seal. The magnitude of this pressure difference is usually maintained at 5 to 10 psi (3.5 to 6.9 N/cm^2).

The cooling air in chamber 6 can leak between the outer rear sideplate and the rear face of the blade base into chamber 12 that is at a pressure slightly higher than the turbine discharge. The cooling air also can leak from chamber 7 through the loose-fitting blade serrations. The pressure level in these regions will be between the turbine rotor inlet and exit static pressures. Air also can leak by the tang at the forward end of the blade base and then between the forward face of the blade base and the forward sideplate. The ambient pressure at this potential leakage point will be slightly higher than the turbine rotor inlet static pressure.

APPARATUS AND INSTRUMENTATION

The test apparatus used for this investigation was designed to use actual engine parts wherever possible. In static tests using this test apparatus, the pressure levels and pressure differences that would exist in and around the test blade cooling-air system during engine operation were duplicated as nearly as possible. There were two main pieces of test apparatus: one to study airflow through a disk-blade assembly and another to study airflow through a blade.

Disk-Blade Airflow and Leakage Studies

Test apparatus. - The test apparatus for the disk airflow study is shown in cross section in figure 3. In this apparatus, a fixture plate was substituted for the seal support plate shown in figure 1 and the turbine disk bolts were extended to provide a firm attachment between the disk assembly (which normally rotates) and the stationary part of the seal assembly. In addition, the labyrinth seal between chamber 4 and chamber 12 was replaced with an O-ring seal to eliminate leakage; a seal ring was interposed between chamber 4 and chamber 3; and a sealed chamber was provided at the centerline of the turbine disk. The airflow into and out of the various air chambers in the apparatus could be controlled independently. For the inner-seal balance air, the test blade cooling air, the outer-seal balance air, and the thrust balance air, this control was accomplished with valves in the supply lines to these chambers. The entry points on the test apparatus for these airflows are designated as ports 1, 2, 3, and 4, respectively, in figure 4. For labyrinth seal leakage-flow tests only (described later) seal strips were installed at the outer radius of the inner rear sideplate (detail B, fig. 3) in order to block the cooling-air flow path to the test blades at port 5. For the serration leakage tests, seal strips were installed at the inlet to the blade bases (detail A, fig. 3). These seal strips prevented cooling air from flowing past port 7.

Airflow system and instrumentation. - The airflow to the test apparatus was controlled and measured by the metering system shown in figure 4. For the full-flow tests, filtered, pressurized room-temperature air flowed through a pressure regulator and a venturi tube before entering the test blade cooling-air annular manifold. The setting of the pressure regulator determined the airflow rates in these tests. For the labyrinth and serration leakage tests, the airflow was directed through another branch of the air-metering system, which contained a pressure regulator, a rotameter, a manual control valve, and a heater. (The heater was used only for serration leakage tests.) This airflow could be introduced into the test apparatus through any of the following ports: test

blade cooling air (port 2), inner seal balance air (port 1), or outer seal balance air (port 3). In the labyrinth seal leakage tests, the airflow exiting from the apparatus was measured with another rotameter. A valve downstream of this exit rotameter determined the back-pressure that was imposed on the airflow exiting from the test apparatus.

Thermocouples and static-pressure taps were located at the venturi tube, the inlet of each rotameter, and downstream of the heater. Within the disk and seal assembly, static-pressure taps were located at the positions shown in figure 4. The static-pressure taps in chambers 1 to 7 were used to sense static pressure levels; the static-pressure taps internal to the two three-stage labyrinth seals were used differentially to sense the pressure drop across the center knife-edge of the seals. Static pressures were read on precision gages to an accuracy of ±0.05 psi (0.03 N/cm^2); pressure differences across the center knife-edges of the labyrinth seals were read on inclined-tube manometers to an accuracy of ±0.01 inch of water (0.0002 N/cm^2).

Blade Airflow Study

Test apparatus. - The test apparatus for the blade airflow study is shown in figure 5. A cooling-air supply tube that simulated the geometry of chamber 7 (fig. 1) was attached and sealed to the base of the blade. At the blade tip, a compartmented collector assembly was attached by a clamping device which was anchored to the blade hub platform. The collector assembly was divided into leading-edge, midchord, and trailing-edge compartments. The open (bottom) end of each compartment was sealed individually to the blade tip. Individual rotameters were used to measure cooling airflow from each compartment of the collector assembly.

Airflow metering and instrumentation. - The airflow metering system for the blade airflow study was similar to that used in the disk-blade airflow study. The blade airflow metering system was described in detail in reference 2. Filtered, pressurized, room-temperature air was directed through a pressure regulator and a rotameter to the cooling-air supply tube at the blade base. A manual control valve and a rotameter were installed in each of the exit lines from the collector assembly. A thermocouple and a pressure tap were installed at the inlet to each rotameter. Static-pressure taps were installed in the supply tube, the blade, and the collector assembly, as shown in figure 5, to measure pressure levels and pressure drops throughout the blade. These taps were located as follows: in the supply tube, one in each of the oblong passages of the blade stalk, one in the stalk-to-airfoil transition section, and one in each of the compartments of the collector assembly. All pressure measurements were read to an accuracy of ±0.05 psi (0.03 N/cm^2).

EXPERIMENTAL PROCEDURE

Disk-Blade Airflow and Leakage Studies

The experimental disk-blade airflow studies were of two types; full-flow tests and leakage-flow tests. In the full-flow tests, cooling air was introduced to the disk, flowed through the disk cooling-air passage, and was discharged from the blade tips. In the leakage-flow tests, the normal exit path through the blade tips was blocked so that flow leakage from various parts of the disk cooling-air passage could be measured. These tests are described below and listed in table I.

Full-flow tests. - The cooling-air pressure drop from the hub of the disk to the base of the test blades was determined by flowing air through the test blade cooling-air system over a range of pressures equal to that which would be encountered during engine operation. This test was designated Series 1 and is described in table I. Air was introduced through the inlet airflow line to the test blade cooling-air manifold (port 2, fig. 4) and flowed through the normal supply route in the rear sideplates to and through the blades. For this series of tests, ports 1, 3, and 4 were sealed. Pressures were measured in chambers 2, 5, and 7 and the room-temperature inlet airflow was measured by the inlet venturi tube. A range of inlet pressure at port 2 from 28 to 100 psi (19 to 69 N/cm^2) was investigated.

Leakage-flow tests. - Leakage flow around the serrated blades and through the labyrinth seal was determined by two series of tests.

Blade serration leakage tests: The blade serration leakage tests are designated Series 2 on table I. For these tests all ports except 2, 5, and 6 were sealed. Therefore, all the air which entered the test apparatus through port 2 exited as leakage from the region of the blade mounting serrations (port 6). In this series of tests, the pressure to which this air leaks was atmospheric. Pressures were measured in chambers 2, 5, and 7, and the airflow was measured by the inlet rotameter. The serration leakage was investigated over a range of pressures from 20 to 100 psia (14 to 69 N/cm^2) and temperatures from 67° to 472° F (293 to 518 K) at station 7.

Labyrinth seal leakage tests: Room-temperature tests were run to determine leakage across the two three-stage labyrinth seals at very low pressure differences (less than 1 in. of water (0.03 N/cm^2) across the center knife-edge at air inlet pressures of 50 and 100 psia (34.5 and 69 N/cm^2)). Because this leakage could be in either direction (i.e., from test blade cooling-air chamber (chamber 2) to pressure-balance chambers (chambers 1 and 3) or conversely) across either seal independently, the test procedure was set up to investigate both cases. These tests are designated series 3 and 4 in table I. Following the nomenclature of reference 3, the flow of air from the test blade cooling-air chamber to the balance chambers (chambers 1 and 3) was defined as

leakage in the normal direction, while airflow into chamber 2 from chambers 1 and 3 was defined as leakage in the reverse direction. All ports in the test apparatus except the inner- and outer-seal balance air ports were closed for the seal leakage tests (see table I). For series 3 tests, the inlet airflow was introduced into the test apparatus through the inner-seal port, flowed into the inner-seal balance (chamber 1, fig. 4) through the three-stage inner labyrinth seal into the test blade cooling-air chamber (chamber 2), through the three-stage outer labyrinth seal into the outer-seal balance chamber (chamber 3), out the outer-seal port, and through the exit rotameter to the atmosphere. In this test, leakage was measured across the inner seal in a reverse direction and across the outer seal in a normal direction. In series 4 tests, the flow path was reversed so that leakage was in a reverse direction across the outer seal and a normal direction across the inner seal. Pressure was measured in chambers 1, 2, and 3 and at the inlets to both rotameters. Pressure drops ranging from zero to 1 inch of water (0 to 0.02 N/cm^2) across the center knife-edge of the seals were investigated at pressure levels of 50 and 100 psia (34.5 and 69 N/cm^2).

Blade Airflow Studies

The pressure level to which the cooling air discharges at the blade tip is not a readily definable quantity. Experimental measurements on the stationary shroud surrounding the turbine blades on an experimental engine indicated that a pressure gradient that closely approximates a linear change between the rotor-inlet static pressure and the rotor-exit static pressure exists along the stationary wall. Because means to make pressure measurements on the rotating blades were not available, the tip discharge pressures at different chordwise locations on the blade could not be defined. To simulate possible pressure distributions that may occur at the blade tips, tests were run over a range of constant blade exit pressures and also over two different pressure gradients. The desired pressure gradients and the constant-pressure conditions imposed at the blade tip were established by adjusting the valves in the exit lines from the leading-edge, midchord, and trailing-edge compartments of the collector assembly to obtain the desired back-pressure. Leading-edge to trailing-edge pressure gradients of 40 to 32 psia and 43 to 27 psia (28 to 22 and 30 to 19 N/cm^2, respectively) were investigated. Constant pressure levels (zero gradient) at the blade tip of 44, 36, and 30 psia (30, 25, and 21 N/cm^2, respectively) were also investigated. The airflow rates were varied from 0.0155 to 0.0475 pound per second (0.0070 to 0.0215 kg/sec). Air temperatures, pressures, and weight flows were recorded for each combination of flow conditions.

ANALYTICAL METHODS FOR CALCULATING PRESSURE CHANGES IN DISK AND BLADE STATIC TESTS

Cooling-air pressure drops in the disk and blade passages were determined analytically. These calculations were made first for static room-temperature conditions and the calculated results were compared with experimental results. Next, the effects of rotation and heat addition were introduced to correct for environmental conditions encountered in engine operation.

The flow of air in the test blade cooling-air system progressed through a series of irregular passages from the hub of the turbine disk to the tip of the blade. Numerous expansions, contractions, and right-angle turns occurred in the direction of flow. Within the disk passages, the flow progressed under the influence of radial pressure gradients. However, in some cases a chordwise pressure gradient at the blade tip caused varying radial pressure gradients within the internal passages of the blade. To account for all the flow perturbations in the disk and blade passages for static, room-temperature airflow conditions, the relations described in the following paragraphs were used to calculate expansion, contraction, and turning losses and other pressure losses due to friction and momentum change.

Pressure Loss Relations

Entrance loss. - The entrance loss (herein defined as the loss in total pressure due to a sudden contraction) may be calculated from the following incompressible flow equation

$$\Delta P = K_{en} \frac{G^2}{2g\rho} \tag{1}$$

where ΔP is the change in total pressure and G is based on conditions in the smaller passage. (Symbols are defined in appendix A.) Since equation (1) was only applied to cooling airflow Mach numbers less than 0.2, the assumption of incompressible flow is acceptable.

Friction pressure change. - The usual equation for the frictional static-pressure change for turbulent flow through a pipe,

$$\Delta p_f = \frac{4fLG_{av}^2}{D_h 2g\rho_{av}} \tag{2}$$

was used, where G_{av} is the average mass flow rate per unit area, D_h is the hydraulic diameter, and ρ_{av} is the average of ρ_{in} and ρ_{out}. Based on experimental data for turbulent flow in smooth tubes, the friction factor f is given empirically in the following equation

$$\frac{f}{2} = 0.023\ (Re)^{-0.2} \tag{3}$$

If the Reynolds number Re in equation (3) is replaced by its definition

$$Re = \frac{GD_h}{\mu} \tag{4}$$

and the resulting equation is substituted into equation (2) with G replaced by $\dot{w}/A$, the following relation between $\rho_{av}\ \Delta p_f$ and $\dot{w}$ results

$$\rho_{av}\ \Delta p_f = \left(\frac{0.092\ L\mu^{0.2}}{A^{1.8} D_h^{1.2} g}\right) \dot{w}^{1.8} \tag{5}$$

Turning loss. - Turning losses can be calculated by using equation (2) with an equivalent L/D based on the turn geometry.

Momentum pressure change. - The momentum static-pressure change may be calculated from

$$\Delta p_m = \frac{G_{av}}{g}\left(\frac{G_{out}}{\rho_{out}} - \frac{G_{in}}{\rho_{in}}\right) \tag{6a}$$

For no area or mass flow rate change, this equation becomes

$$\Delta p_m = \frac{G^2}{g}\left(\frac{1}{\rho_{out}} - \frac{1}{\rho_{in}}\right) \tag{6b}$$

Exit loss. - The exit loss, defined as the total-pressure drop resulting from a sudden enlargement, may be calculated from

$$\Delta P = \frac{(1 - \epsilon)^2 G^2}{2g\rho} \tag{7}$$

where ϵ is the ratio of the upstream flow area to the downstream flow area and G and ρ are based on conditions just upstream of the exit.

Disk-Blade Airflow Studies

Figure 6 shows the flow path of the cooling air from the hub of the disk to the base of the blade. By dividing this flow path into segments that could be analyzed separately, the changes in static and total pressures were calculated in a stepwise fashion. Using the equations given in the preceding paragraphs, pressure changes from the disk hub (chamber 2) to the blade base (chamber 7) were calculated at each of the stations designated in figure 6. A description of the disk passages at each station is given in table II.

To calculate pressure changes in the disk passages for static, room-temperature conditions, the measured static pressure, temperature and weight flow rate at station 2a were used as a starting point. The temperature was assumed to be constant throughout the disk passages at 80° F (300 K). The airflow rate was constant from the disk hub (station 2a) to the maximum radius of the outer rear sideplate passage (station 6e). At this point, one-third of the calibrated serration leakage was deducted from the airflow. The remaining two-thirds of the serration leakage was assumed to escape between stations 7a and 7b and between station 7b and the forward sideplate. The allocation of the serration is arbitrary. However, the exact allocation of the serration leakage is not critical, as will be seen later.

Where required, static and total pressures were related by

$$P = p\left(1 + \frac{\gamma - 1}{2} M^2\right)^{\gamma/(\gamma-1)} \tag{8}$$

Using equations (1) to (8), values for P and p were calculated at each station between 2a and 7b, as shown on table III.

Blade Airflow Studies

The airflow through the blades was treated in two steps. From the blade inlet air supply tube to the stalk-to-airfoil transition section, the flow was assumed to divide evenly in the two-blade stalk passages. From the transition section to the blade tip, the flow was influenced either by a chordwise pressure gradient or by a constant pressure at the blade tip and was distributed accordingly.

Pressure drop from supply tube to transition section. - The steps required to calculate the pressure drop from point 7b to point 9 are summarized in table III. The static pressure in the transition section was calculated by using the measured inlet supply tube static pressure and equations (1) to (8) to determine flow around a bend, entrance loss due to contraction, friction pressure drop, and exit loss due to an expansion.

Pressure drop from transition section to tip collectors. - Attempts to theoretically predict static-pressure distributions in the blade leading-edge, midchord, and trailing-edge passages were not successful due to the fact that these parallel passages were interconnected and the effect of crossflow between these passages was difficult to determine theoretically. Therefore, the pressure drop for this portion of the blade was presented as a correlation between the $\rho\ \Delta p$ and the coolant flow rate. This correlation is discussed in the following section.

RESULTS AND DISCUSSION

Disk-Blade Airflow and Leakage Studies

Full-flow tests (series 1). - The variation of airflow through the test blade cooling-air system with pressure drop parameter $(\rho_{av}\ \Delta p)_{2a\text{-}7b}$, is shown in figure 7. The pressure drop Δp in this parameter is the pressure change from station 2a to station 7b. The density ρ_{av} is based on the average of the pressures measured at stations 2a and 7b. The total flow rate is that measured at station 2a.

Leakage-flow tests. - Two series of leakage-flow tests were made: serration leakage tests and labyrinth seal leakage tests.

Serration leakage (series 2): The data obtained from the serration leakage tests are presented in figure 8 as weight flow against a pressure drop parameter. These tests were made over a range of air temperatures from 67° to 472° F (293 to 519 K). An attempt to assess the effect of viscosity was made by cross-plotting the data of figure 8 as flow rate against viscosity. A slope of -0.5 was obtained from this cross-plot, and the pressure drop parameter of figure 8 was modified by the viscosity raised to the -0.5 power to obtain figure 9. It is noted that the viscosity correction to the pressure drop

parameter, while improving the correlation, did not completely eliminate the temperature effects. It is possible that thermal expansion between blade and disk mating surfaces may contribute to the data scatter.

Balanced-pressure labyrinth seal leakage (series 3 and 4): Experimentally determined leakage-flow rates across the three-stage balanced-pressure outer labyrinth seal are shown in figure 10. These data were obtained from test series 3 and 4. The figure is equally applicable to the inner seal when the proper area is used in the weight flow parameter. Also shown in this figure are the analytically determined flow rates across an ideal labyrinth seal. An ideal labyrinth seal is defined here as a seal in which the kinetic energy of the leakage flow is completely converted into heat following each labyrinth stage. The method of reference 4 was used to correlate these data. The slope of the line through the experimental data agrees with the slope of the ideal-seal-leakage line but is displaced on the weight flow parameter axis by a factor of 1.5. The data of reference 3 are plotted also in figure 10 for comparison with the present seal. The test seal in reference 3 was similar in design to the present seal but had a knife-edge spacing of 0.75 inch (1.9 cm) compared to 0.375 inch (0.95 cm) for the present seal. The diameter of the seal land of reference 3 was 14.8 inches (37.6 cm) compared to 4.4 inches (11 cm) for the present seal. The data for the seal of reference 3 are displaced on the weight-flow parameter axis of figure 10 by a factor of 1.25. For a given temperature pressure, leakage area, and pressure drop, it has been shown in reference 4 that leakage flow through a labyrinth seal of the type tested herein is a function of the number of knife-edges and the gap-to-knife-edge spacing ratio. (Gap is defined as the radial distance between the land and the knife-edge on a labyrinth seal; spacing is the axial distance between knife-edges.) A flow correction factor of 1.42 is shown in reference 4 for a seal with a gap-to-spacing ratio of 0.066 (present seal); a correction factor of 1.27 is shown for a seal with a gap-to-spacing ratio of 0.033 (seal of ref. 3). These values compare favorably with the indicated correction factors of figure 10.

Comparison of measured and calculated pressures at the blade base. - Static pressures were measured experimentally at stations 2a, 2f, 5a, and 7b during the disk-blade airflow studies. Using the measured pressure at station 2a as a starting point, static pressures were calculated for stations 2f, 5a, and 7b by the method described in the analytical methods section. Since external leakage paths are sealed by O-rings, there was no leakage either into or out of the blade cooling airflow through the three-stage balanced-pressure labyrinth seals. The serration leakage for the cold flow static tests are generally about 10 percent of the total cooling air flow. The comparisons of calculated and measured pressures are shown in figure 11. Figure 11(a) shows that the agreement between measured and calculated pressures for stations 2f and 5a was very good. Figure 11(b) shows that calculated pressures at station 7b were slightly higher than the measured pressures over the entire pressure range. The diamond symbols

indicate the calculated pressures assuming that one-third of the serration leakage occurred before the cooling airflow reached station 7a. The triangular symbols indicate calculated pressures assuming no serration leakage. This comparison showed that the arbitrary allocation of serration leakage previously assumed is not critical to the calculation of cooling pressure changes. Because the calculated pressures based on either leakage assumption showed insignificant differences, the no-leakage assumption is chosen for the engine application for simplicity. In general, the difference between measured and calculated pressures was about 3 percent of the pressure level. The comparison on figure 11(b) shows that the pressure at the blade base can be calculated with reasonable accuracy for the static, room-temperature case by a stepwise treatment of the flow path as a series of expansion, contraction, and frictional losses.

Blade Airflow Studies

Pressure drop from air supply tube-to-transition section. - With the measured pressure in the air supply tube p_7, the static pressure in the transition section at the airfoil hub p_9 was calculated as described in the analytical methods section. These calculated pressures are compared with the pressures actually measured at this point in figure 12. Excellent agreement was obtained with maximum differences of approximately 1 percent between calculated and measured values of p_9. The pressure drop parameter $\rho_{av} \Delta p_{7b-9}$ from the air supply tube to the transition section is shown in figure 13 as a function of cooling airflow. The pressure drop was based on measured pressures in the air supply tube and the transition section. The density term in the pressure drop parameter was based on an average of the air supply tube and transition section pressures. For all cases, the data correlated within about 5 percent.

Pressure drop parameter from transition section to tip collectors. - Figure 14 is based on measured collector flow rates and transition section and tip collector pressures The density is calculated from the average of the transition section and the collector pressures. Figures 14(a) to (c) show the pressure drop parameter plotted against the measured collector flow rate for the blade leading-edge, midchord and trailing-edge regions, respectively. Figure 14(a) shows that the pressure drop parameter plotted against the flow rate measured in the blade leading-edge collector is affected by the pressure gradient maintained across the blade tip region, especially for very low flow rates. For the constant-collector-pressure cases, the data correlate linearly on the log-log plot of figure 14(a). As the leading-edge collector pressure is increased, the values of $(\rho_{av} \Delta p)_{9-11}$ for the gradient cases increase over those for the constant-collector-pressure cases for the same values of measured leading-edge collector flow rates, becoming almost flat at the highest collector pressure investigated. Figure 14(a)

shows that, as the leading-edge flow rate increases, the curves representing the different blade exit pressure conditions converge.

Figures 14(b) and (c), for the midchord and trailing-edge regions, respectively, show linear correlations for all the data regardless of the collector pressure gradients considered. However, for these regions, the collector flow rates were in the range where the leading-edge region curves converged (see fig. 14(a)).

Comparison of single-blade and five-blade cascade airflow results. - A comparison of results from the single-blade airflow studies and from the disk - blade assembly airflow studies was made on the basis of the pressure drop parameter from the air supply tube to the blade tip. (The atmospheric pressure at the blade tip in the disk airflow tests corresponds to the collector pressures measured in the blade airflow tests.) To obtain this correlation, values of $(\rho_{av}\ \Delta p)_{9\text{-}11}$ were assumed, and flow rates through the three blade passages were read from the correlation curves of figures 14(a) to (c). For figure 14(a), the linear curve was used, since the pressure at the blade tip was constant in the disk airflow tests. The three values of the flow rates read from figures 14(a) to (c) for an assumed value of $(\rho_{av}\ \Delta p)_{9\text{-}11}$ were added to give the total flow rate through the blade. Using this total flow rate, a value of $(\rho_{av}\ \Delta p)_{7b\text{-}9}$ was then read from figure 13. By adding $(\rho_{av}\ \Delta p)_{7b\text{-}9}$ to the assumed value of $(\rho_{av}\ \Delta p)_{9\text{-}11}$, a value of $(\rho_{av}\ \Delta p)_{7b\text{-}11}$ was obtained for each assumed value of $(\rho_{av}\ \Delta p)_{9\text{-}11}$ and the result plotted against the total flow rate. The circular symbols in figure 15 represent these values.

The square symbols in figure 15 were obtained from disk - blade assembly airflow data corrected for serration leakage. The total flow rate through five blades, the static pressures at the blade base, and the ambient (atmospheric) pressure at the blade tips were measured, and the density was evaluated as the average of the supply tube and atmospheric pressures. Values of $(\rho_{av}\ \Delta p)_{7b\text{-}11}$ were then calculated from measured pressures and plotted against the flow rate through one blade (one-fifth of the measured flow rate, corrected for serration leakage, through the five-blade pack). Figure 15 shows excellent agreement between the data obtained from the two separate airflow studies. The agreement also indicates the serration leakage calibration is valid.

APPLICATION OF STATIC, ROOM-TEMPERATURE AIRFLOW RESULTS TO DATA FROM ENGINE OPERATION

When heat-transfer tests are performed using the research engine, it will be necessary to know the flow distribution within the blade in order to predict blade metal temperatures. The coolant static pressure, temperature, and flow rate at the base of the blade, station 7b, can be calculated based on application of cold flow static tests on the

turbine wheel disk. The coolant pressure, temperature, and flow rate at the blade base, together with the experimental flow data from the static blade airflow studies, can be used to calculate the flow distribution through the blade.

To apply the results of the static, room-temperature airflow studies to data obtained during engine operation, the effects of pumping due to rotation and momentum changes from heat addition to the cooling air must be considered. The pumping effect can be accounted for by including the rotation terms defined in the following equation in the calculation of cooling-air pressure in the engine:

$$\Delta p_{\omega} = \frac{\rho_{av}\, \omega^2\, (r_{out}^2 - r_{in}^2)}{2g} \tag{9}$$

The momentum pressure changes due to coolant flow area change and coolant temperature rise can be calculated from equation (6a). The application of the disk and blade airflow static tests results to the calculation of blade coolant flow distribution will be discussed in detail in the following paragraphs.

Disk Airflow

During engine operation the coolant static pressure, temperature, and flow rate are known at station 2a on the stationary parts of the seal assembly. The pressure at the base of the blade can be calculated using the measured static pressure at station 2a as a starting point. The stepwise procedure described for static, room-temperature conditions can be modified to include the effects of momentum change and rotation in the calculation of pressure drops under engine operating conditions. For engine application the airflow rate at station 2b should be adjusted for labyrinth seal leakage. The leakage adjustment can be based on cold flow seal calibrations, as shown in figure 10. From station 2b to the maximum radius of the outer rear sideplate passage (station 6e), the airflow rate will be constant. For the purpose of determining the pressure at the blade base, the serration leakage between stations 6e and 12 was neglected, therefore, the airflow can also be considered constant between these two stations. This was done because as was shown in the section RESULTS AND DISCUSSION the serration leakage was not critical to the calculation of cooling-air pressure at the blade base.

The temperature of the cooling air will be affected by environmental conditions along the flow path. Compression due to rotation will result in an attendant rise in cooling air temperature, but this temperature rise will be small in the research engine and may be neglected. The temperature of the cooling air can be assumed to be constant from point 2a to station 6a since the temperatures of the airflows directed to the inner

seal, the outer seal, the test blades, and the thrust-balance chamber are approximately equal. In addition, the cooling air which flows up the forward face of the turbine disk to cool the slave blades was approximately the same temperature as the airflows bathing the rear face. From point 6a to point 6e, the cooling air can be assumed to be in contact with metal at a temperature that is a mean value between the air temperature at point 6a and the environmental temperature in chamber 12. The coolant temperature rise from station 6a to 6e can be calculated from the following equation, which was derived assuming that the metal temperature, coolant heat capacity, and wall-to-coolant convective-heat-transfer coefficient were constant along the passage:

$$\frac{T_m - T_{in}}{T_m - T_{out}} = \exp\left(\frac{hA_{ht}}{\dot{w}C_p}\right) \tag{10}$$

where h can be determined by the method of W. M. Kays as described on pages 175 to 180 in reference 5 since the passage aspect ratio ranges from approximately 10 to 25. The coolant temperature at station 7b can be assumed equal to the coolant temperature at station 6e. The temperatures obtained from equation (10) can be used to calculate the coolant densities required in equations (1) to (9). The stepwise procedure shown in table IV can then be used to calculate the pressure at station 7b.

Blade Airflow Studies

Calculation of pressure drop from inlet supply tube to transition section. - Since figure 13 shows that, for static conditions, the method used to calculate p_9 in the static tests was quite accurate, the same procedure modified to include rotational effects can be used to calculate p_9 for the engine tests. The stepwise calculations indicated in table IV can be used to determine the pressure at station 9. The cooling-air temperature rise from station 7b to 9 can be calculated by using equation (10) and the assumption that the blade metal temperature is approximately equal to the rotor disk temperature in this area. The convective-heat-transfer coefficient in the stalk passages can be obtained from the following equation:

$$h = 0.023 \frac{k}{D_h} \left(\frac{GD_h}{\mu}\right)^{0.8} \left(\frac{\mu C_p}{k}\right)^{0.4}$$

Calculation of pressure drop from transition section to engine shroud. - As mentioned previously in the analytical procedures section a stepwise calculation through each

part of the blade from the transition section to the engine shroud similar to that just described from the inlet supply tube to the blade plenum was not possible. Consequently, a correlation based on an overall pressure drop parameter from the blade plenum to the engine shroud can be used to predict the coolant flow distribution in the blade leading-edge, midchord, and trailing-edge passages. In order to use figure 14 to predict coolant exit flow from these passages, the pressure drop parameter $(\rho_{av}\ \Delta p)_{9\text{-}11,e}$ determined from measurements obtained during engine tests must be modified to correspond to the cold flow test pressure drop parameter $(\rho_{av}\ \Delta p)_{9\text{-}11,s}$ which was obtained during static airflow tests.

If it is assumed that

(1) One velocity head loss in total pressure occurs at the blade tip

(2) The friction pressure drop parameter $\rho_{av}\ \Delta p_f$ in a given blade airfoil passage is the same for the engine tests as it was for the blade airflow tests

(3) The entrance loss coefficient from the transition section to a given blade airfoil passage entrance is not a function of rotational velocity or coolant temperature

then it can be shown that the following relation applies:

$$(\rho_{av}\ \Delta p)_{9\text{-}11,s} = (\rho_{av}\ \Delta p)_{9\text{-}11,e} - (\rho_{av}\ \Delta p)_{10a\text{-}10b,m,e} + (\rho_{av}\ \Delta p)_{9\text{-}11,\omega,e} \tag{11}$$

The derivation of this relation is given in appendix B. The evaluation of all terms in equation (11) is also described in appendix B.

Calculation of flow distribution in blade airflow. - The airflow rate in the leading-edge passage can be determined from figure 14(a). An interpolation may be required if the blade tip pressure is not constant or if the existing gradient does not equal either of the two gradients investigated. The airflow rate in the midchord and trailing-edge passages can be determined from the single curves on figures 14(b) and (c). The total exit cooling flow through the blade during engine tests can be obtained by summing the calculated flow through the individual blade passages. If this total calculated flow does not equal the measured coolant flow supplied to the disk at station 2a minus the labyrinth and serration leakages, the individual coolant exit flows should be normalized based on measured flowrate corrected for labyrinth seal and serration leakages. For the purpose of predicting blade metal temperatures that occur during engine tests, the flow distribution through a given blade passage can be assumed to vary linearly from an area prorated flow at the blade hub to the calculated flow at the blade tip.

In order to assess the magnitude of the serration leakage relative to the total coolant flow, the pressure at the blade base was calculated according to the analytical method presented, using a typical engine research run data. The serration leakage was determined from figure 9, using the calculated blade base pressure, the measured blade

base temperature, and the measured blade base external pressure. The engine data used were

Engine speed, rpm	8100
Static pressure, psia (N/cm^2):	
At station 2a (calculated)	88.2 (60.8)
At station 7b (calculated)	84.5 (58.3)
At station 12	16.7 (11.5)
Temperature, ^{o}R (K):	
At station 2a	1332 (740)
At station 7b	1339 (744)

The calculated serration leakage was 0.033 pound per second (0.015 kg/sec). Since the total coolant flow was 0.22 pound per second (0.1 kg/sec), the leakage represented about 15 percent of the total coolant flow.

The 15-percent serration leakage, obtained from static calibration and applied to the engine, does not necessarily represent typical serration leakage in turbojet engines. This is because the pressure difference between the blade base internal and external pressures in the research engine is considerably higher than those used in typical turbojet engines. However, it does indicate that the serration leakage can constitute a significant portion of the total test blade coolant flow. The leakage does not significantly affect the calculated pressure at the blade base. But the leakage will decrease the cooling-air flow to the test blades.

The exact serration leakage in the engine is difficult to assess because of the pressure gradient surrounding the blade serration and because of the unknown effects of temperature and rotation on the leakage flow area. Therefore, when the blade coolant flow rate is based on flow measurement at a stationary location, corrected by statically calibrated leakage flow rates such as the serration leakage and the labyrinth seal leakage, the accuracy of the corrected flow depends on how well these calibrations duplicate the engine conditions.

CONCLUDING REMARKS

The results of the static, room-temperature airflow study on a disk-blade assembly and of an individual blade airflow study reported herein can be summarized as follows:

1. Pressure changes in the cooling-air flow path of a disk-blade assembly can be accurately predicted for static, room-temperature conditions by the use of established relations to account for expansion, contraction, turning, and frictional losses in the flow

path. Comparisons of measured and calculated cooling-air pressure changes from the hub of the disk to the base of the blade agreed favorably.

2. Detailed study of airflow from the blade base to the blade transition section also resulted in good agreement between measured and calculated pressure changes. Although theoretical predictions of pressure distributions through the three-blade airfoil cooling passages (leading-edge, midchord, and trailing-edge) were not successful, the flow exiting through each radial blade cooling passage was correlated with the pressure drop parameter.

3. The calibrated leakage of a three-stage balanced-pressure labyrinth seal that was an integral part of the cooling-air flow path agreed well with theoretically predicted leakage for very low pressure differences across the seal.

4. On the basis of the demonstrated comparisons between measured and calculated results for static, room-temperature conditions, an expanded analytical procedure was proposed for application to engine operating conditions that would account for rotation and the change in momentum due to heat addition, as well as the expansion, contraction, turning, and frictional losses.

Lewis Research Center,
National Aeronautics and Space Administration,
Cleveland, Ohio, December 2, 1970,
720-03.

APPENDIX A

SYMBOLS

A	passage area
C_p	specific heat
D_h	hydraulic dyameter
f	friction factor
G	mass flow rate per unit area
g	acceleration due to gravity
h	heat-transfer coefficient
K	loss coefficient
k	thermal conductivity
L	length
M	Mach number
P	total pressure
p	static pressure
Re	Reynolds number
r	radial distance from engine centerline
T	temperature
$\dot{w}$	mass flow rate
γ	ratio of specific heats
ϵ	ratio of upstream to downstream flow area
μ	viscosity
ρ	density
ω	rotational speed
1 to 12	chamber ports in airflow system

Subscripts:

av	average
e	engine tests
en	entrance
ex	exit
f	friction
ht	heat transfer
in	passage inlet
le	leading edge
M	metal
m	momentum
mc	midchord
s	static airflow tests
sl	serration leakage
out	passage outlet
u	upstream
ω	rotation
1 to 12	station designation

APPENDIX B

DERIVATION OF EQUATIONS FOR RELATING STATIC AIRFOIL PRESSURE DROP PARAMETER TO ENGINE DATA

Pressure Drop in Cold Flow Tests

The static pressure drop in cold flow static tests is

$$\Delta p_{9\text{-}11,\,s} = \Delta p_{9\text{-}10a,\,en,\,s} + \Delta p_{10a\text{-}10b,\,f,\,s} + \Delta p_{10a\text{-}10b,\,m,\,s} + \Delta p_{10b\text{-}11,\,ex,\,s} \tag{B1}$$

Assuming a 1-velocity-head loss from the blade tip to the exit flow collector and since the blade passage areas and cooling-air density do not change appreciably from hub to tip, the last two terms of equation (B1) can be assumed negligible. Equation (B1) then becomes

$$\Delta p_{9\text{-}11,\,s} = \Delta p_{9\text{-}10a,\,en,\,s} + \Delta p_{10a\text{-}10b,\,f,\,s} \tag{B2}$$

Pressure Drop During Engine Tests

An equation similar to equation (B1) can be written for the pressure drop from the blade transition section to the engine shroud static-pressure-tap location for the engine tests.

$$\Delta p_{9\text{-}11,\,e} = \Delta p_{9\text{-}10a,\,en,\,e} + \Delta p_{10a\text{-}10b,\,f,\,e} + \Delta p_{10a\text{-}10b,\,m,\,e} + \Delta p_{10b\text{-}11,\,ex,\,e} - \Delta p_{9\text{-}11,\,\omega,\,e} \tag{B3}$$

Again assuming a 1-velocity-head exit loss at the blade tip, equation (B3) becomes

$$\Delta p_{9\text{-}11,\,e} = \Delta p_{9\text{-}10a,\,en,\,e} + \Delta p_{10a\text{-}10b,\,f,\,e} + \Delta p_{10a\text{-}10b,\,m,\,e} - \Delta p_{9\text{-}11,\,\omega,\,e} \tag{B4}$$

Pressure drop parameter equations. - In order to apply the cold flow data given in figure 16, to engine tests, equations (B2) and (B4) can be written in terms of the pressure drop parameter $\rho\,\Delta p$ as follows:

$$(\rho_{av}\,\Delta p)_{9\text{-}11,s} \cong (\rho_{10a}\,\Delta p)_{9\text{-}10a,en,s} + (\rho_{av}\,\Delta p)_{10a\text{-}10b,f,s} \tag{B5}$$

$$(\rho_{av}\,\Delta p)_{9\text{-}11,e} - (\rho_{av}\,\Delta p)_{10a\text{-}10b,m,e} + (\rho_{av}\,\Delta p)_{9\text{-}11,\omega,e}$$

$$\cong (\rho_{10a}\,\Delta p)_{9\text{-}10a,en,e} + (\rho_{av}\,\Delta p)_{10a\text{-}10b,f,e} \tag{B6}$$

Based on the results of reference 2, it appears that the pressure drop term for typical air-cooled passages in turbine hardware is not a strong function of coolant temperature. Therefore, for the purpose of this analysis it will be assumed that

$$(\rho_{av}\,\Delta p)_{10a\text{-}10b,f,s} = (\rho_{av}\,\Delta p)_{10a\text{-}10b,f,e}$$

The right sides of equations (B5) and (B6) therefore, differ by only the $(\rho_{10a}\,\Delta p)_{9\text{-}10a,en,s}$ and $(\rho_{10a}\,\Delta p)_{9\text{-}10a,en,e}$ terms. However, it can be shown as follows that these terms are approximately equal if it is assumed that the entrance loss coefficient K_{en} is not a function of temperature. If the entrance loss coefficients for the engine and static, room-temperature disk-blade assembly tests are equated, the following equation is obtained after some rearrangement.

$$\frac{(\rho_{10a}\,\Delta p)_{9\text{-}10a,en,e}}{\frac{1}{2}(G_{10a})_e^2} - \frac{(\rho_{10a}\,\Delta p)_{9\text{-}10a,en,s}}{\frac{1}{2}(G_{10a})_s^2} = \left(\frac{\dot{w}_9}{\dot{w}_{10a}}\right)_s^2 \left(\frac{A_{10a}}{A_9}\right)_s^2 \left(\frac{\rho_{10a}}{\rho_9}\right)_s$$

$$- \left(\frac{\dot{w}_9}{\dot{w}_{10a}}\right)_e^2 \left(\frac{A_{10a}}{A_9}\right)_e^2 \left(\frac{\rho_{10a}}{\rho_9}\right)_e \tag{B7}$$

Assuming the same coolant flow and entrance geometry for the engine and cold flow tests, equation (B7) can be written as

$$(\rho_{10a}\,\Delta p)_{9\text{-}10a,en,e} - (\rho_{10a}\,\Delta p)_{9\text{-}10a,en,s} = \frac{G_9^2}{2}\left(\frac{\Delta p_{9\text{-}10a,en,e}}{p_9} - \frac{\Delta p_{9\text{-}10a,en,s}}{p_9}\right) \tag{B8}$$

since $\Delta p_{9\text{-}10a,en,s}/p_9$ and $\Delta p_{9\text{-}10a,en,e}/p_9$ are small terms, their difference is even smaller and the right side of equation (B8) is approximately equal to zero. Therefore,

$$(\rho_{10a}\ \Delta p)_{9\text{-}10a,en,e} \cong (\rho_{10a}\ \Delta p)_{9\text{-}10a,en,s}$$

It has, therefore, been shown that the right side of equations (B5) and (B6) are approximately equal and the terms on the left side of equation (B6) can, therefore, be used as the value of $(\rho_{av}\ \Delta p)_{9\text{-}11,s}$ to determine coolant flows at the blade tip from figure 14.

Evaluation of pressure drop parameter. - Before the left side of equation (B6) can be used as the ordinate of figure 14 to determine the exit cooling flow from the blade passages at the blade tip, all terms on the left side of the equation must be evaluated. The $(\rho_{av}\ \Delta p)_{9\text{-}11,e}$ term can be readily obtained from the calculated blade transition section static pressure and the appropriate shroud static pressure (depending on the blade passage being considered); ρ_{av} is the average of the densities at stations 9 and 11. If the coolant temperature rise through the blade is assumed linear, the coolant temperature at station 11 can be determined by assuming that the coolant temperature rise from the transition section to the blade tip is twice the coolant temperature rise from the blade transition section to midspan (midspan cooling-air temperature will be measured during engine tests). The momentum pressure drop parameter $(\rho_{av}\ \Delta p)_{10a\text{-}10b,m,e}$ can be calculated using the following equation, where ρ_{av} and G_{av} are average values between stations 10a and 10b:

$$(\rho_{av}\ \Delta p)_{10a\text{-}10b,m,e} = \frac{\rho_{av}\ G_{av}}{g}\left(\frac{G_{10b}}{\rho_{10b}} - \frac{G_{10a}}{\rho_{10a}}\right)_e \tag{B9}$$

The average coolant density in a given passage can be assumed equal to the average density used in calculating the $(\rho_{av}\ \Delta p)_{9\text{-}11,e}$ term. The calculation of the coolant temperature at the blade tip has already been discussed. The coolant flow rate at the airfoil inlet can be based on prorating the total flow on a passage area basis. This recommendation is based on cold flow tests which gave a minimum of data scatter when entrance losses from the blade transition section to the airfoil inlet were calculated based on prorating the coolant flow on a passage area basis. The coolant flow at station 10b for each blade passage must be eventually determined from figure 14. The rotational term in equation (B6) can be calculated using the following equation:

$$(\rho_{av}\ \Delta p)_{9\text{-}11,\omega,e} = \frac{\rho_{av}^2\ \omega^2\ (r_{10b}^2 - r_9^2)}{2g} \tag{B10}$$

where ρ_{av} is the average density between stations 9 and 11. Since the unknown exit flow at the blade tip appears as a term in equation (B9), an iterative solution is required.

REFERENCES

1. Calvert, Howard F.; Cochran, Reeves P.; Dengler, Robert P.; Hickel, Robert O.; and Norris, James W.: Turbine Cooling Research Facility. NASA TM X-1027, 1970.

2. Clark, John S.; Richards, Hadley T.; Poferl, David J.; and Livingood, John N. B.: Coolant Pressure and Flow Distribution Through an Air-Cooled Vane for a High-Temperature Gas Turbine. NASA TM X-2028, 1970.

3. Yeh, Frederick C.; and Cochran, Reeves P.: Comparison of Experimental and Ideal Leakage Flows Through Labyrinth Seals for Very Small Pressure Differences. NASA TM X-1958, 1970.

4. Egli, A.: The Leakage of Steam Through Labyrinth Seals. Trans. ASME, vol. 57, no. 3, Apr. 1935, pp. 115-122.

5. Kays, W. M.: Convective Heat and Mass Transfer. McGraw-Hill Book Co., Inc., 1966.

TABLE I. - DESCRIPTION OF DISK-BLADE AIRFLOW AND LEAKAGE TESTS

[Refer to fig. 4 for location of ports.]

Test series	Description	Inlet and exit ports							Air temperature	
		Inner seal (port 1)	Test blade (port 2)	Outer seal (port 3)	Thrust balance (port 4)	Disk mid-radius (port 5)	Blade serrations (port 6)	Blade base (port 7)	°F	K
1	Cooling air pressure drop	Sealed	Open, inlet	Sealed	Sealed	Open	Open	Open, exit	80	300
2	Blade serration leakage	Sealed	Open, inlet	Sealed	↓	Open	Open, exit	Sealed	67 to 472	293 to 518
3	Balanced-pressure seal leakage	Open, inlet	Sealed	Open, exit	↓	Sealed	Inactive	Inactive	80	300
4	Balanced-pressure seal leakage	Open, exit	Sealed	Open, inlet	↓	Sealed	Inactive	Inactive	80	300

TABLE II. - DISK-BLADE AIRFLOW

PASSAGE DESCRIPTION

Station	Description
2a	Annulus, axial flow
2b	Annulus, axial flow
2c	Peripheral slot, radial flow
2d,e	Twenty-four radial holes, radial flow
2f	Peripheral slot, radial flow
2g	Twenty-four rectangular slots, radial flow
5a	Peripheral slot, radial flow
5b	Peripheral slot, radial flow
5c	Peripheral slot, radial flow
5d	Toroidal cross section, circular flow
5e	Peripheral slot, radial flow
6a,b	Two rectangular slots, radial flow
6c,d	Rectangular slot, radial flow
6e	Annular arc, axial flow
7a,b,c	Five trapezoids, axial flow
8a,b	Rectangular slot, radial flow
9	Transition section, stalk to airfoil
10a	One rectangular and two triangular passages per blade
10b	One rectangular and two triangular passages per blade

TABLE III. - ANALYTICAL PREDICTION OF PRESSURES IN STATIC, ROOM-TEMPERATURE DISK-BLADE ASSEMBLY AND INDIVIDUAL BLADE COOLING-AIR FLOW STUDIES

Station	Calculate total pressure P from equation -	Calculate static pressure p from equation -
2a	(8)	(a)
2b	(7)	(8)
2c	(b)	(b)
2d	(1)	(8)
2e	(8)	(2)
2f	(7)	(8)
2g	(1)	↓
5a	(7)	↓
5b	(1)	↓
5c	(7)	↓
5d	(8)	(2)(assuming two 90° turns, L/D = 60 for each)
5e	(8)	(2)(assuming L/D = 60)
6a	(1)	(8)
6b	(8)	(2)
6c	(7)	(8)
6d	(8)	(2)
6e	(8)	(2)(assuming L/D = 60)
7a	(1)	(8)
7b	(8)	(2)
7c	(8)	(2)(assuming L/D = 60)
8a	(1)	(8)
8b	(8)	(2)
9	(7)	(8)

[a]Measured.

[b]$P_{2c} = P_{2b}$.

TABLE IV. - DISK AND BLADE CALCULATION OF PRESSURES UNDER ENGINE OPERATING CONDITIONS

Station	Calculate total pressure P from equation -	Calculate static pressure p from equation -
2a	(8)	(a)
2b	(7)	(8)
2c	(8)	(9)
2d	(1)	(8)
2e	(8)	(2), (6), (9)
2f	(7)	(8)
2g	(1)	(8)
5a	(7)	[b](8), (9)(from stations 2e to 5a)
5b	(1)	[b](8), (9)
5c	(1)	[b](8), (9)
5d	(8)	(2)(L/D = 60 for two 90° turns)
5e	(8)	(2)(L/D = 60)
6a	(1)	(8)
6b	(8)	[b](2), (6), (9)
6c	(7)	[b](8), (9)
6d	(8)	[b](2), (6), (9)
6e	(8)	(2)(L/D = 60)
7a	(1)	(8)
7b	(8)	(2)
7c	(8)	[b](2)(L/D = 60), (9)
8a	(1)	(8)
8b	(8)	[b](2), (6), (9)
9	(7)	[b](8), (9)
9 to 11	(c)	(c)

[a]Measured.

[b]Since these equations are coupled, an iterative solution is required.

[c]See section of this report on application of results to engine data.

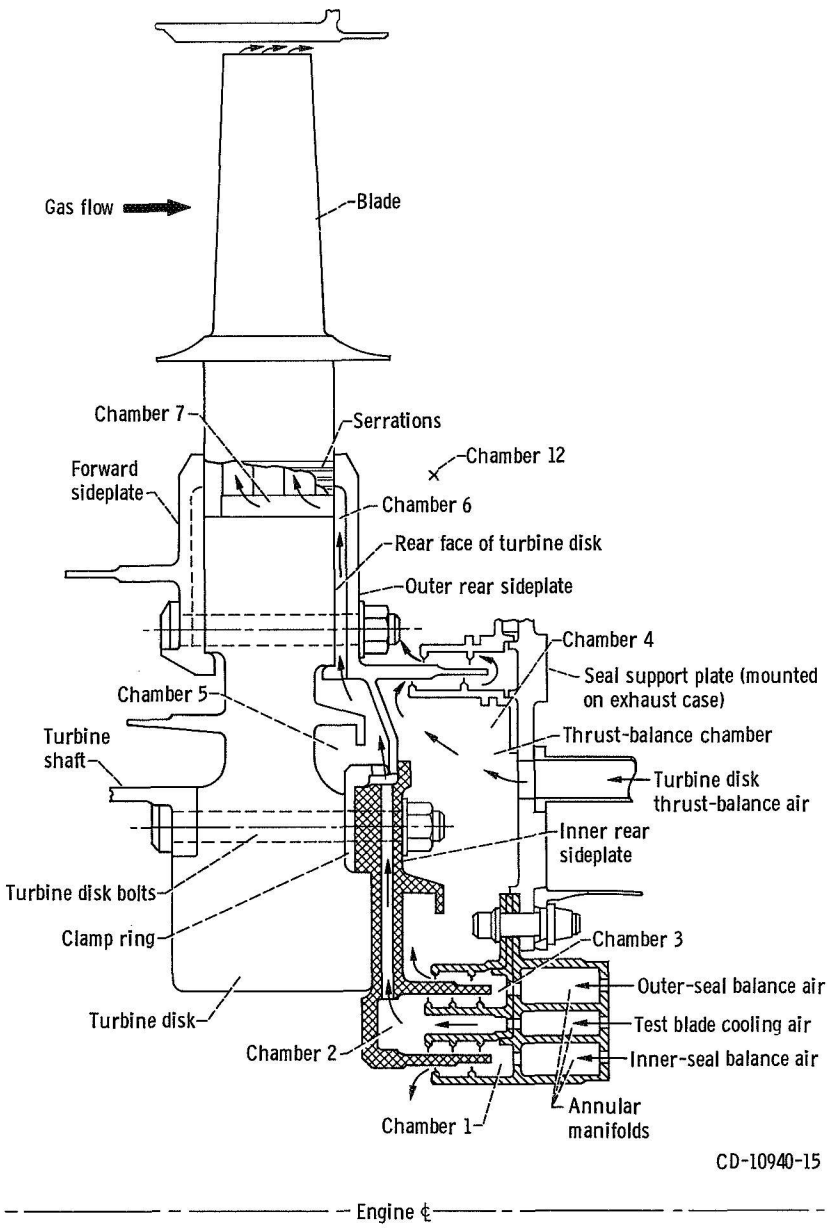

Figure 1. - Schematic of cooling-air flow path through rotor disk and blade of research engine of reference 1.

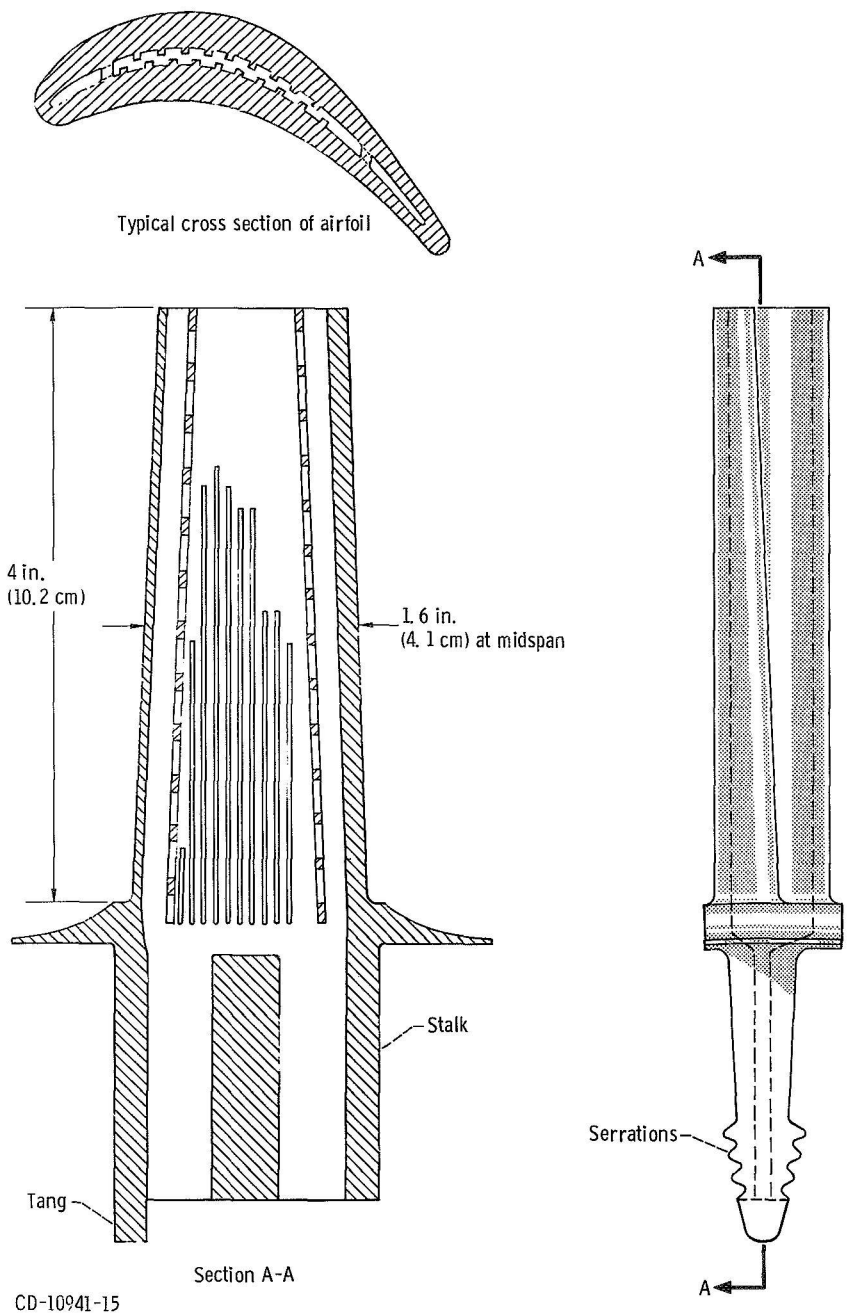

Figure 2. - Details of cooling-air passages on test blade.

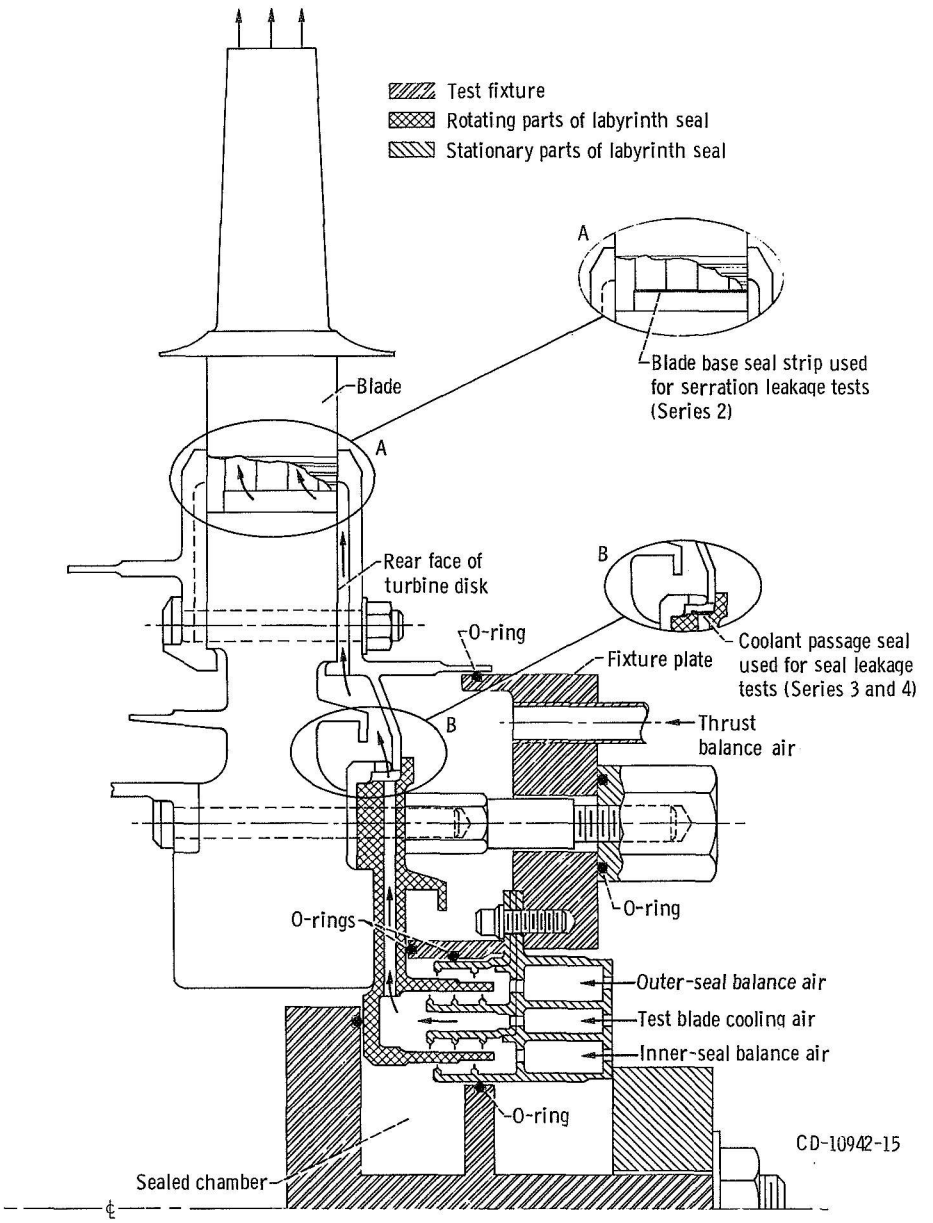

Figure 3. - Test apparatus for disk-blade assembly airflow studies.

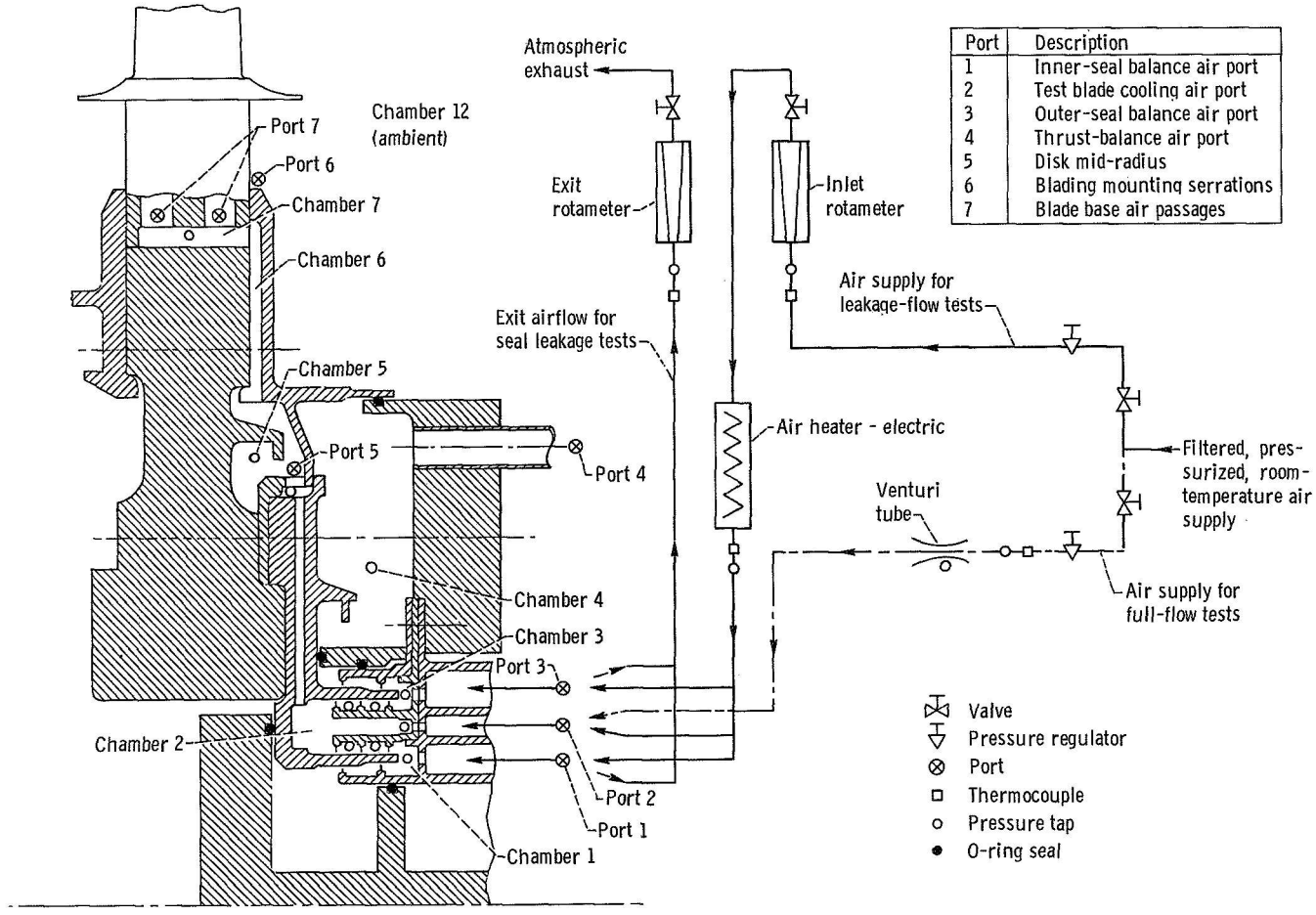

CD-10943-15

Figure 4. - Schematic diagram of air-metering system and instrumentation for disk-blade assembly airflow studies.

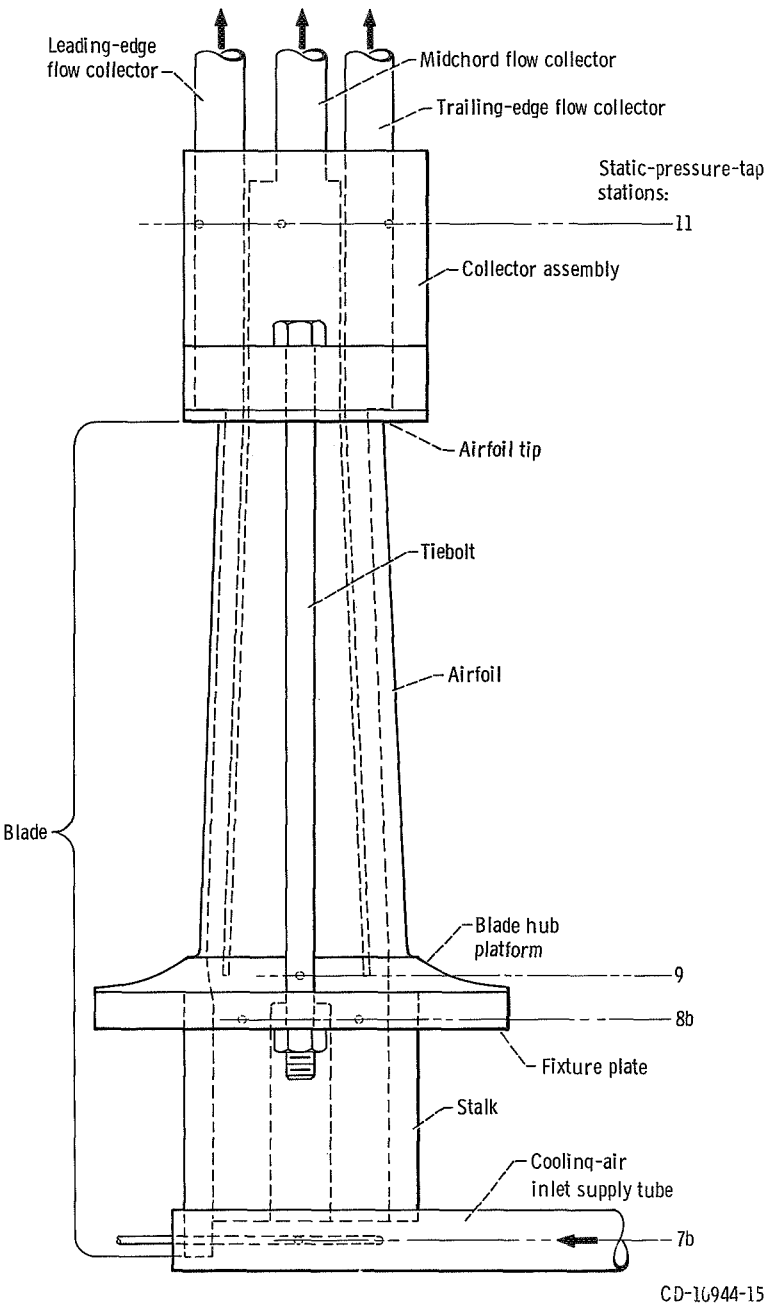

Figure 5. - Flow collectors, pressure instrumentation, and method of attachment for blade airflow studies.

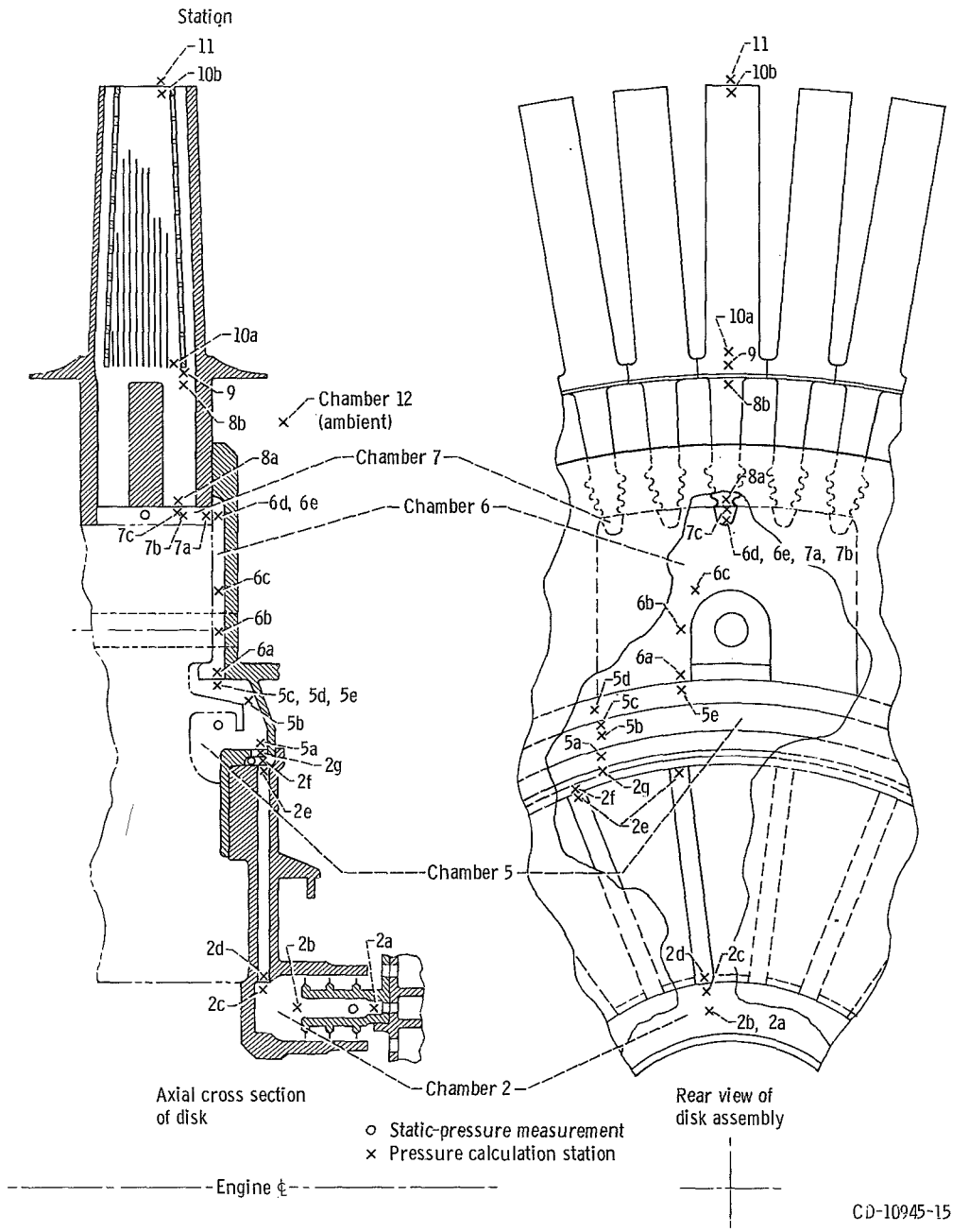

Figure 6. - Schematic diagram of airflow path in disk-blade assembly airflow studies, showing station locations.

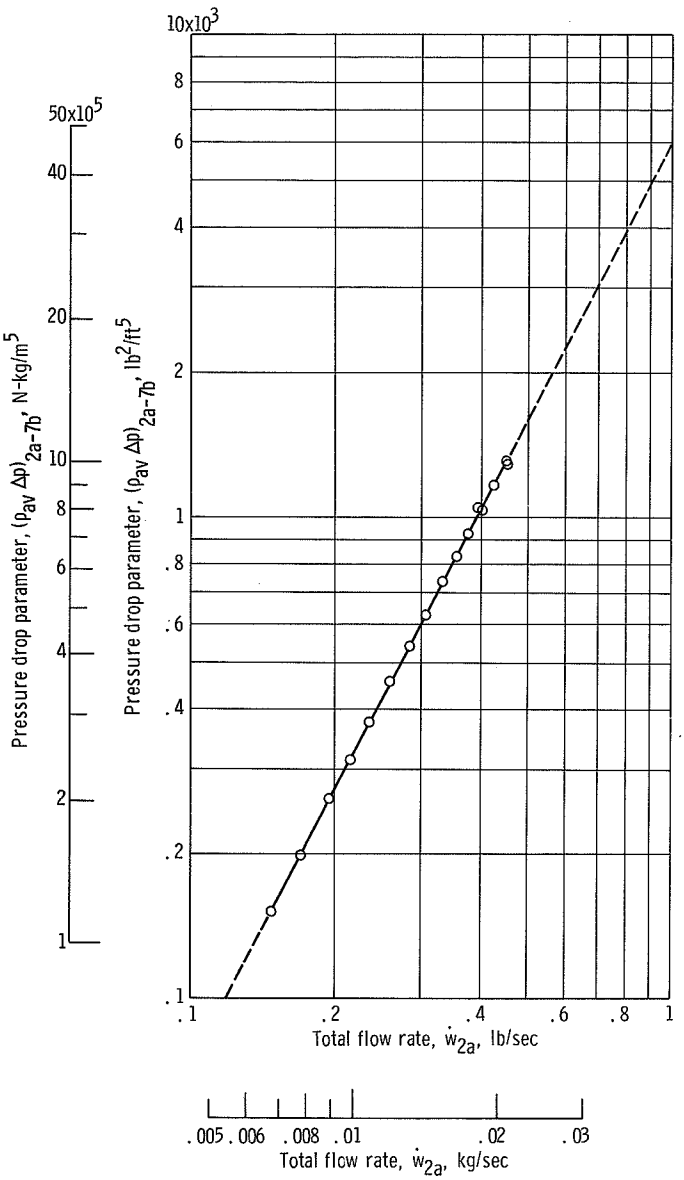

Figure 7. - Pressure drop parameter as function of weight flow rate from disk hub to blade base in disk - blade assembly airflow studies. (Series 1.)

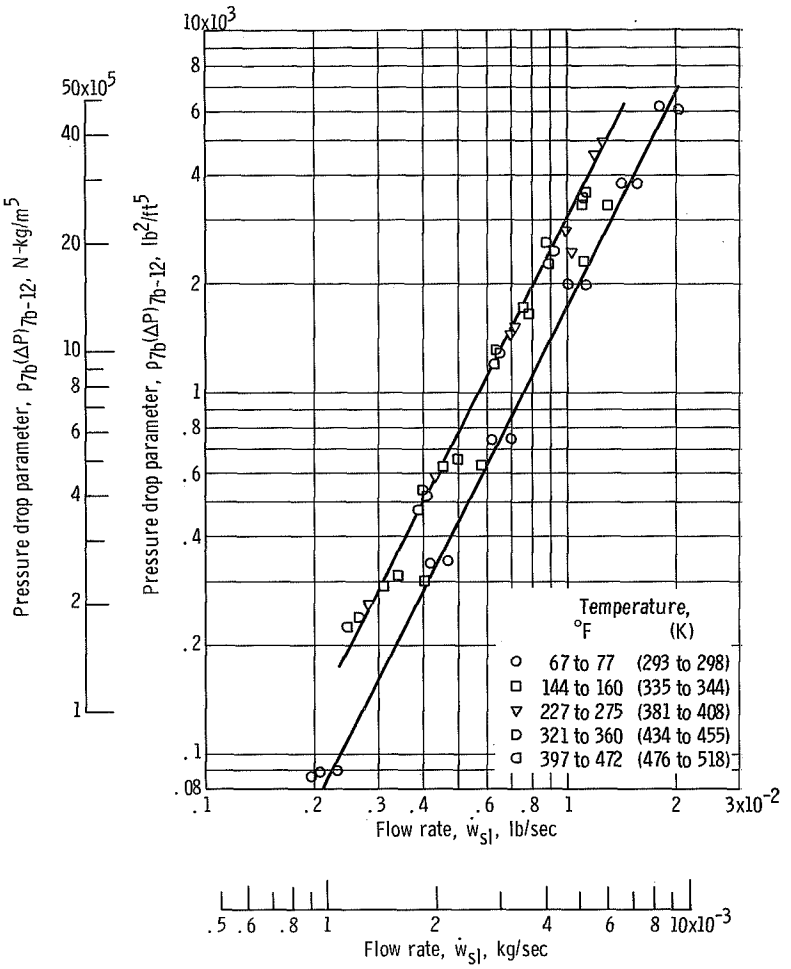

Figure 8. - Pressure drop parameter as a function of serration leakage flow in disk - blade assembly airflow studies (series 2).

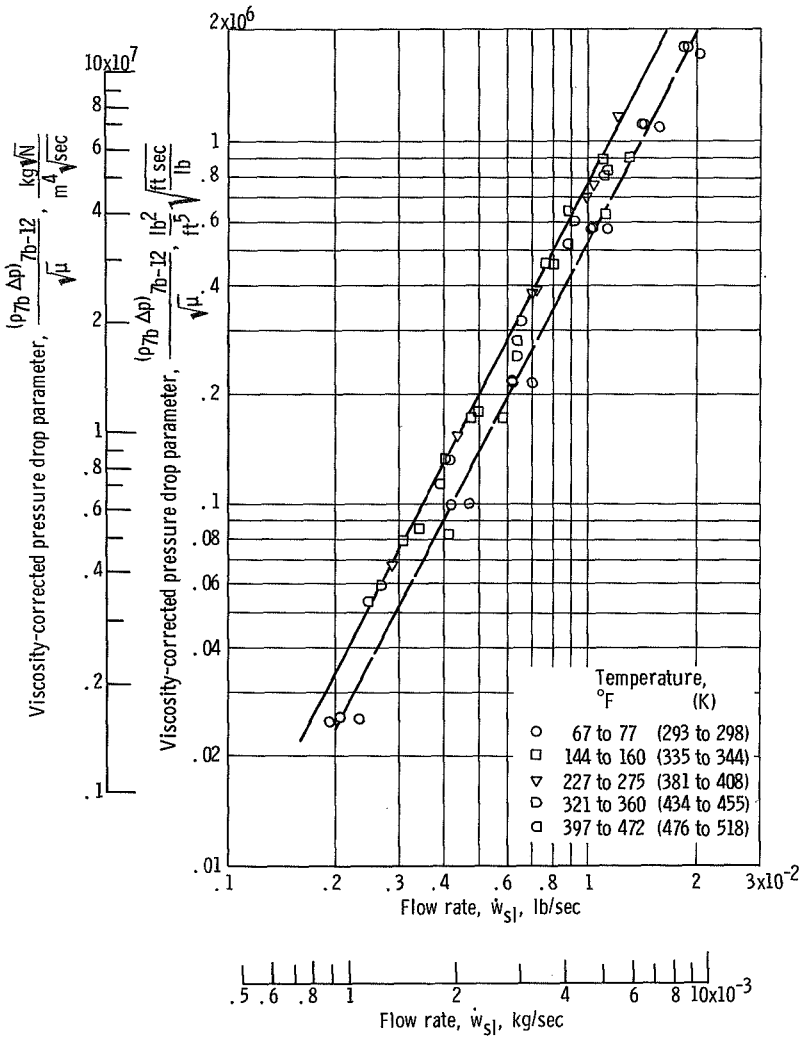

Figure 9. - Viscosity-corrected pressure drop parameter as function of serration leakage flow in disk - blade assembly airflow studies (series 2).

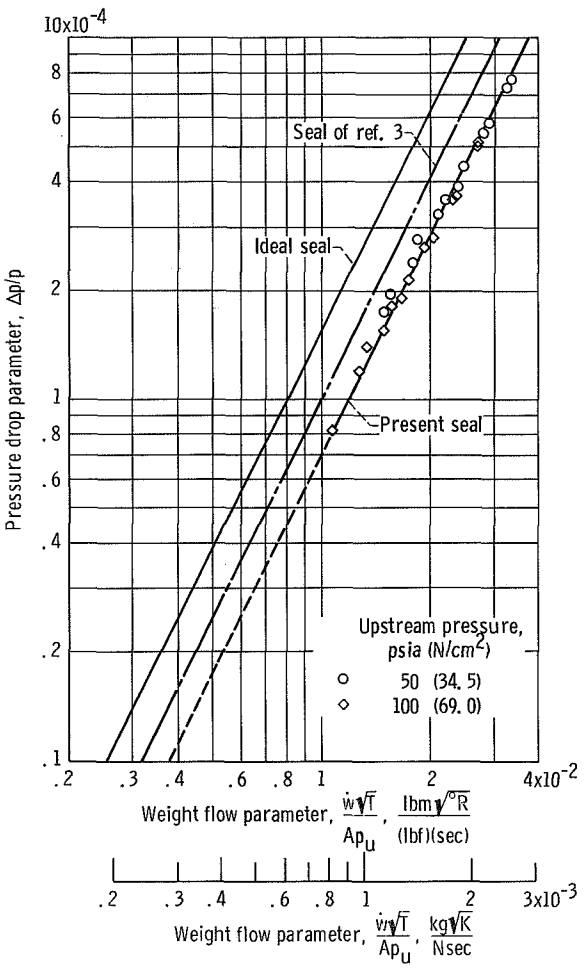

Figure 10. - Pressure drop parameter as function of labyrinth seal leakage flow parameter in disk - blade assembly airflow studies (series 3 and 4).

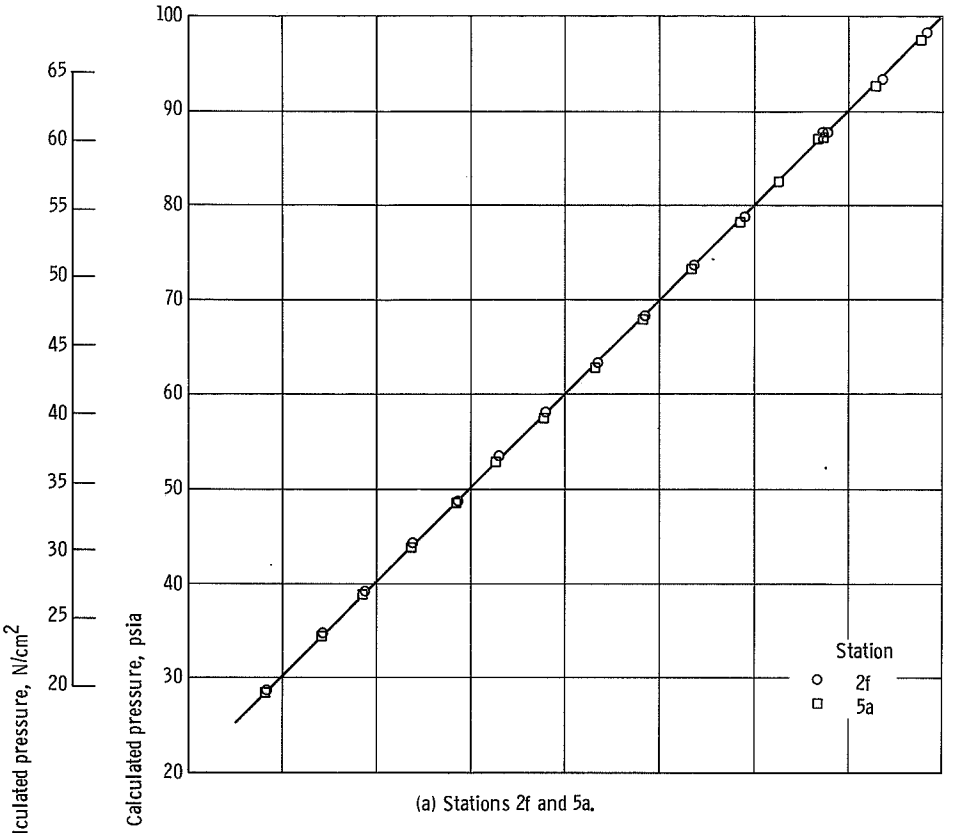

(a) Stations 2f and 5a.

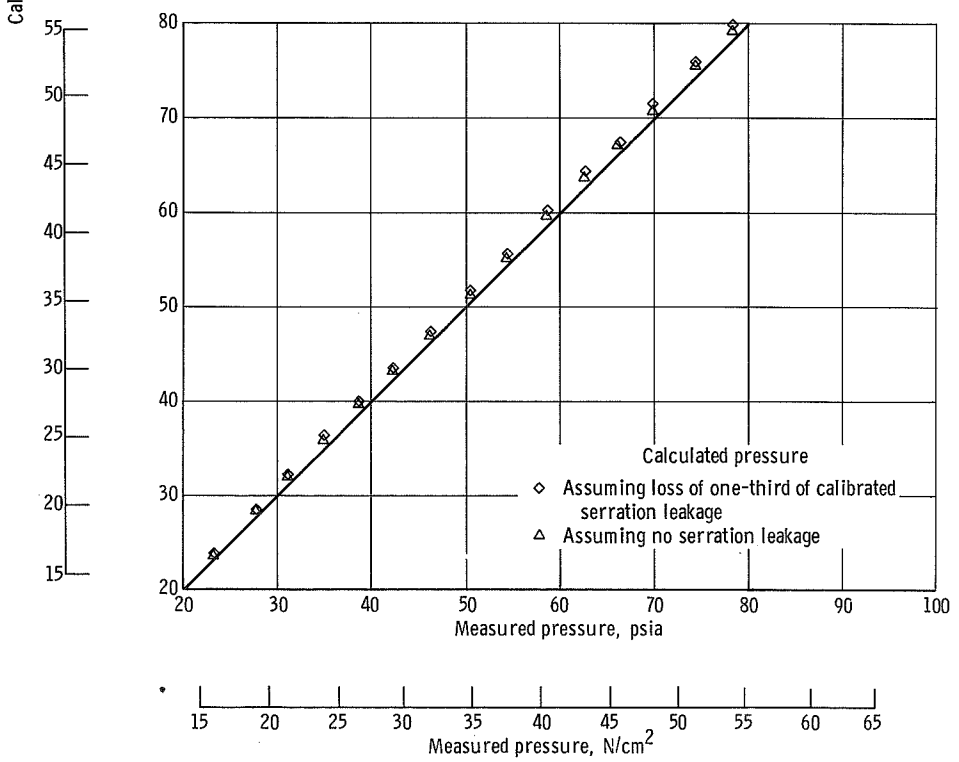

(b) Blade base, station 7b.

Figure 11. - Comparison of measured and calculated pressures in disk airflow studies.

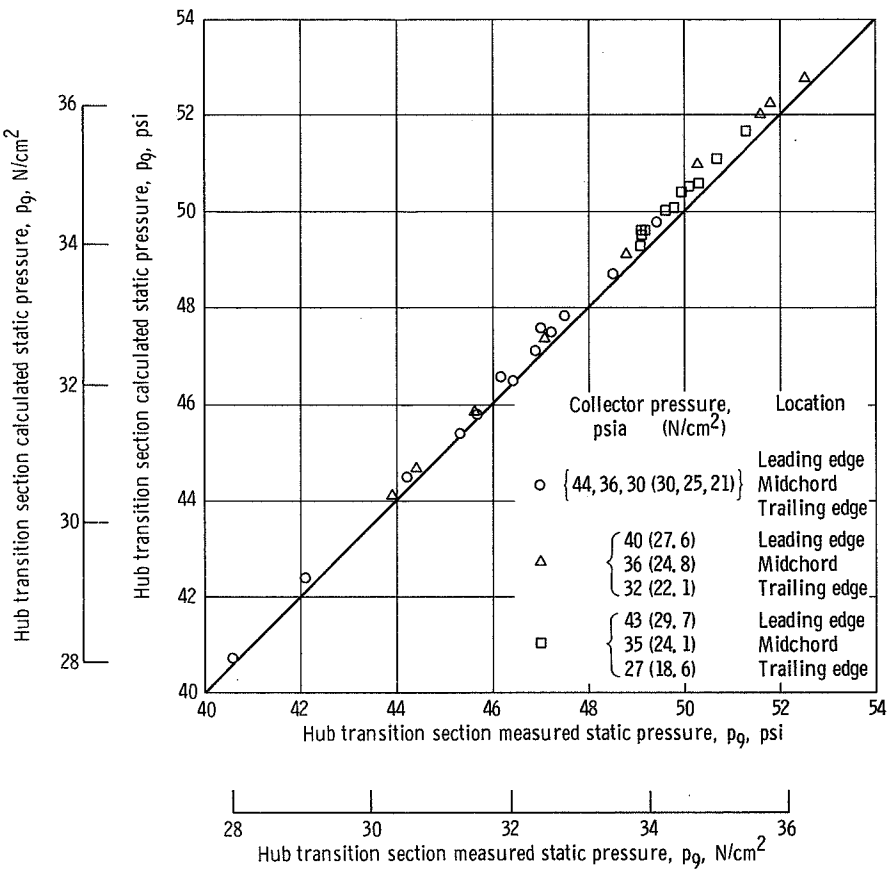

Figure 12. - Comparison of calculated and measured blade hub transition section static pressures for single-blade airflow studies.

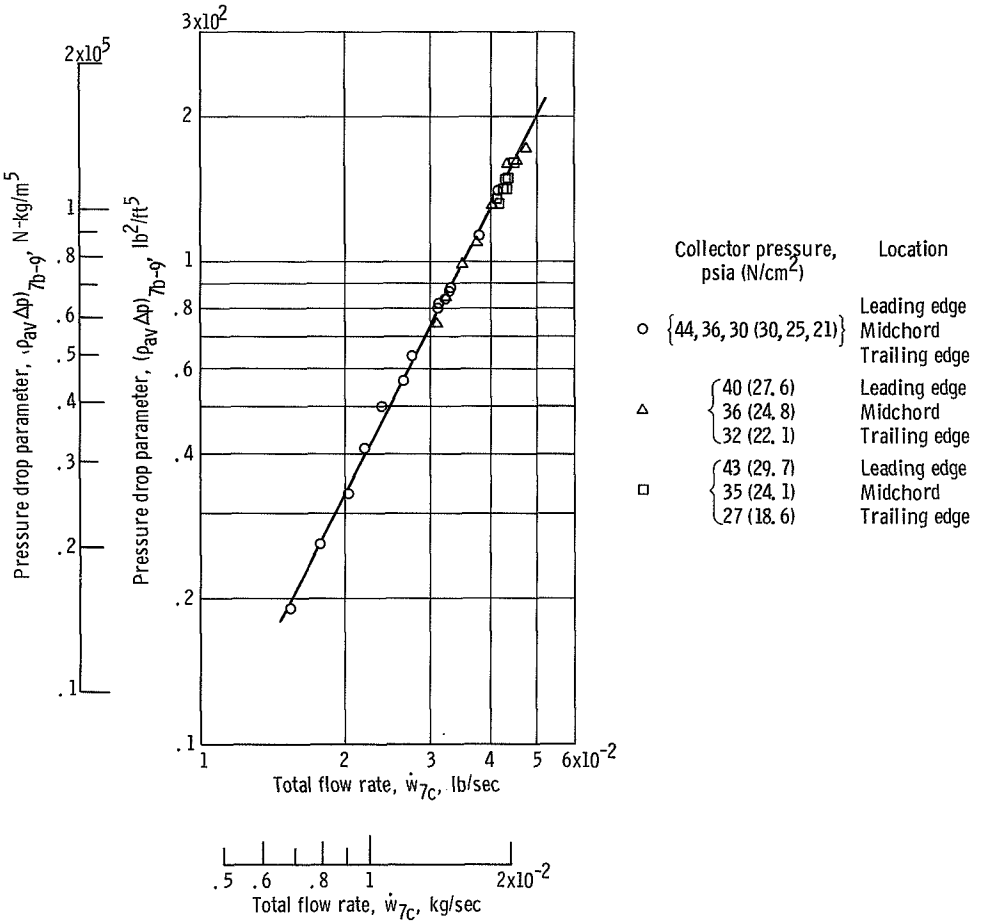

Figure 13. - Pressure drop parameter from station 7b to station 9 as function of flow rate for various values of collector pressures in single-blade airflow studies.

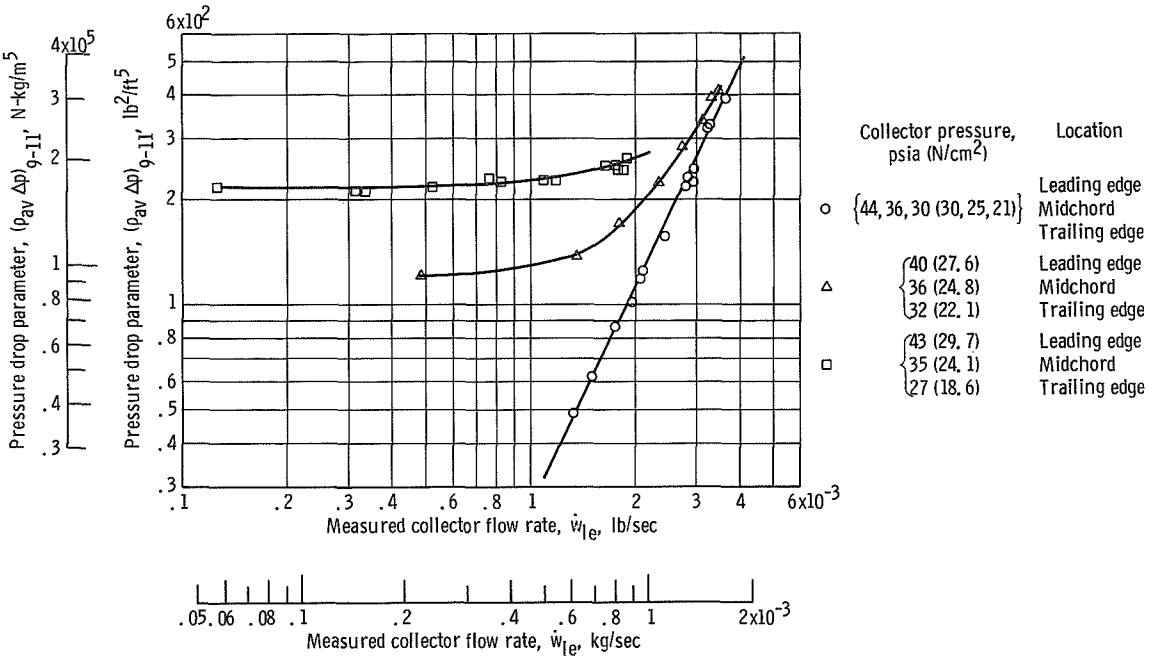

(a) Leading-edge region.

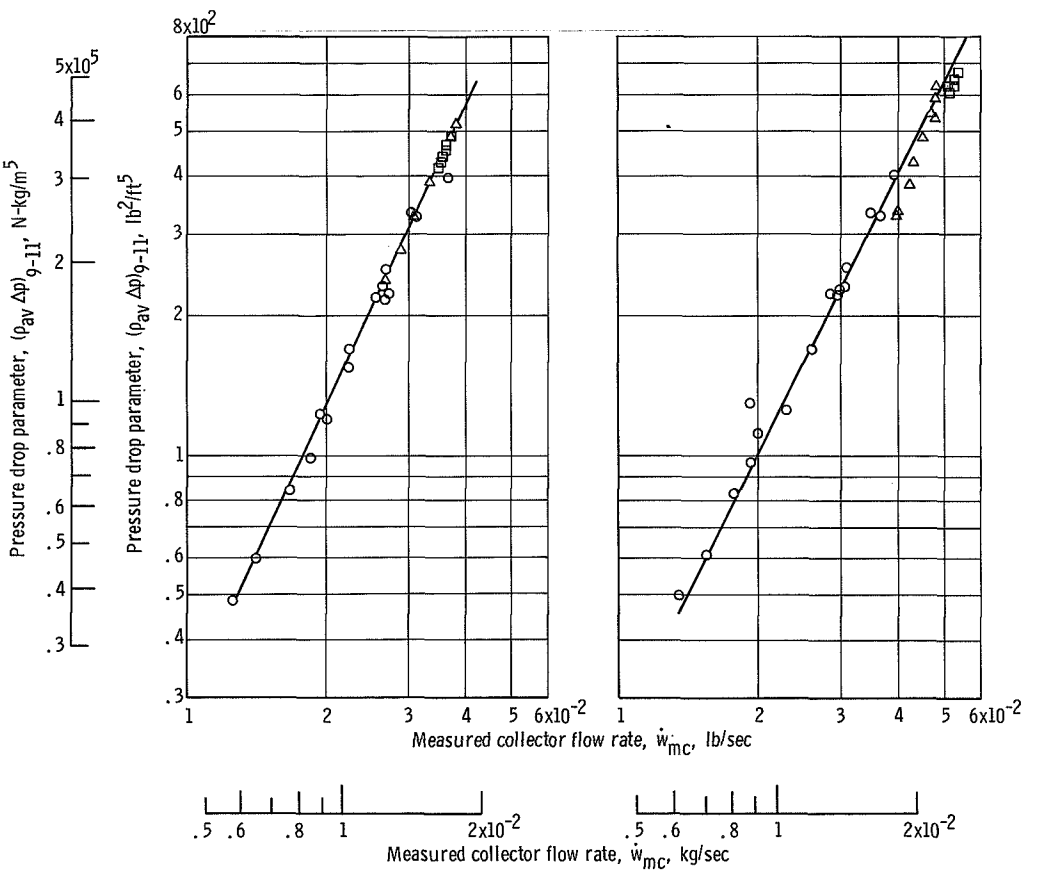

(b) Midchord region.

(c) Trailing-edge region.

Figure 14. - Pressure drop parameter as function of flow rate for various values of tip collector pressures in individual collector compartments in single-blade airflow studies.

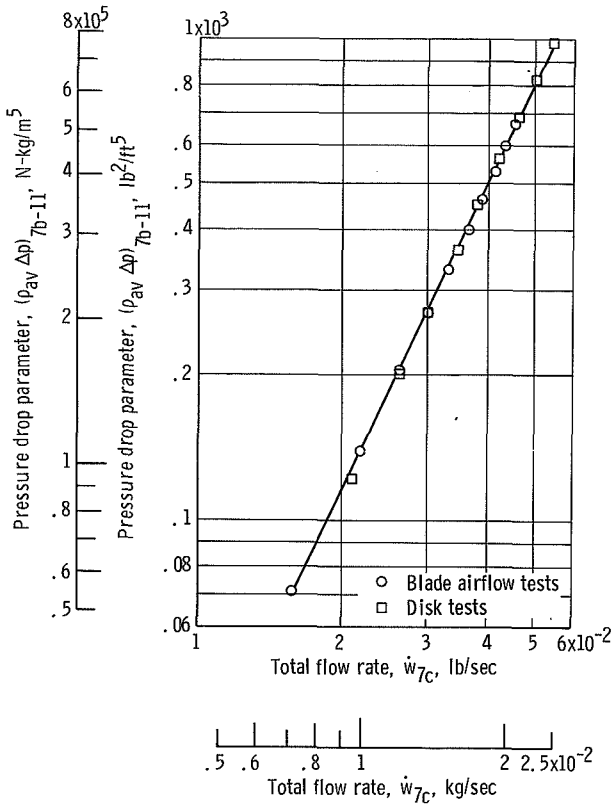

Figure 15. - Comparison of blade pressure drop parameters for disk - blade assembly and single-blade flow tests.

NATIONAL AERONAUTICS AND SPACE ADMINISTRATION
WASHINGTON, D.C. 20546

OFFICIAL BUSINESS
PENALTY FOR PRIVATE USE $300

FIRST CLASS MAIL

POSTAGE AND FEES PAID
NATIONAL AERONAUTICS AND
SPACE ADMINISTRATION

POSTMASTER: If Undeliverable (Section 158
Postal Manual) Do Not Return

"The aeronautical and space activities of the United States shall be conducted so as to contribute . . . to the expansion of human knowledge of phenomena in the atmosphere and space. The Administration shall provide for the widest practicable and appropriate dissemination of information concerning its activities and the results thereof."

—NATIONAL AERONAUTICS AND SPACE ACT OF 1958

NASA SCIENTIFIC AND TECHNICAL PUBLICATIONS

TECHNICAL REPORTS: Scientific and technical information considered important, complete, and a lasting contribution to existing knowledge.

TECHNICAL NOTES: Information less broad in scope but nevertheless of importance as a contribution to existing knowledge.

TECHNICAL MEMORANDUMS: Information receiving limited distribution because of preliminary data, security classification, or other reasons.

CONTRACTOR REPORTS: Scientific and technical information generated under a NASA contract or grant and considered an important contribution to existing knowledge.

TECHNICAL TRANSLATIONS: Information published in a foreign language considered to merit NASA distribution in English.

SPECIAL PUBLICATIONS: Information derived from or of value to NASA activities. Publications include conference proceedings, monographs, data compilations, handbooks, sourcebooks, and special bibliographies.

TECHNOLOGY UTILIZATION PUBLICATIONS: Information on technology used by NASA that may be of particular interest in commercial and other non-aerospace applications. Publications include Tech Briefs, Technology Utilization Reports and Technology Surveys.

Details on the availability of these publications may be obtained from:

SCIENTIFIC AND TECHNICAL INFORMATION OFFICE

NATIONAL AERONAUTICS AND SPACE ADMINISTRATION

Washington, D.C. 20546